Journal of *Marine Science and Engineering*

MDPI

Article

New Seismoacoustic Data on Shallow Gas in Holocene Marine Shelf Sediments, Offshore from the Cilento Promontory (Southern Tyrrhenian Sea, Italy)

Gemma Aiello [1,*] and Mauro Caccavale [1,2]

[1] Institute of Marine Sciences (ISMAR), National Research Council of Italy (CNR), 80133 Naples, Italy
[2] Istituto Nazionale di Geofisica e Vulcanologia (INGV), Sezione Osservatorio Vesuviano (OV), Via Diocleziano 328, 80125 Naples, Italy
* Correspondence: gemma.aiello@cnr.it

Abstract: High-resolution seismoacoustic data represent a useful tool for the investigations of gas-charged sediments occurring beneath the seabed through the identification of the diagnostic intrasedimentary features associated with them. Acoustic blanking revealed shallow gas pockets in the seismostratigraphic units of the inner shelf off the Northern Cilento promontory. Six main seismostratigraphic units were recognized based on the geological interpretation of the seismic profiles. Large shallow gas pockets, reaching a lateral extension of 1 km, are concentrated at the depocenter of Late Pleistocene–Holocene marine sediments that are limited northwards by the Solofrone River mouth and southwards by the Licosa Cape promontory. A morphobathymetric interpretation, reported in a GIS environment, was constructed in order to show the main morphological lineaments and to link them with the acoustic anomalies interpreted through the Sub-bottom chirp profiles. A newly constructed workflow was assessed to perform data elaboration with Seismic Unix software by comparing and improving the seismic data of the previously processed profiles that used Seisprho software. The identification of these anomalies and the corresponding units from the offshore Cilento promontory represent a useful basis for an assessment of marine geohazards and could help to plan for the mitigation of geohazards in the Cilento region.

Keywords: high-resolution seismic profiles; shallow gas; seismic processing; acoustic anomalies; Cilento promontory; Southern Tyrrhenian Sea

check for updates

Citation: Aiello, G.; Caccavale, M. New Seismoacoustic Data on Shallow Gas in Holocene Marine Shelf Sediments, Offshore from the Cilento Promontory (Southern Tyrrhenian Sea, Italy). *J. Mar. Sci. Eng.* **2022**, *10*, 1992. https://doi.org/10.3390/jmse10121992

Academic Editor: Antoni Calafat

Received: 28 November 2022
Revised: 6 December 2022
Accepted: 13 December 2022
Published: 14 December 2022

Publisher's Note: MDPI stays neutral with regard to jurisdictional claims in published maps and institutional affiliations.

Copyright: © 2022 by the authors. Licensee MDPI, Basel, Switzerland. This article is an open access article distributed under the terms and conditions of the Creative Commons Attribution (CC BY) license (https://creativecommons.org/licenses/by/4.0/).

1. Introduction

Reflection seismics is an important tool for shallow-gas investigations as it provides a rapid mean for detecting and mapping gas accumulations [1–4]. Over the last decades, high-resolution seismic exploration data (sub-bottom and Sparker) have been very useful for shallow-gas evaluations [5–7] (among others).

Shallow gas pockets are often limited upwards by a strong seismic reflector, totally masking the underlying sediments, which look absolutely transparent. Acoustically transparent zones that are well shown by high-resolution reflection profiles are often related to gas-charged sediments [8,9]. Hovland and Judd [8] have described in detail the acoustic anomalies related to gas occurrence. Various seismic signatures of gas within sediments have been recognized, including acoustic blanking, bright spots, and enhanced reflections. For the aims of our paper, the most significant acoustic anomaly is acoustic blanking. The reflection or absorption of acoustic energy by gas prevents the recording of reflections from lower sediment layers. Although acoustic blanking is widespread on several of the world's continental margins, it is not always found in close association with pockmarks [8].

The acoustic anomalies related to the occurrence of gas within the sedimentary record have been studied in detail, both in the central Adriatic Sea [10] and in the central Mediterranean Sea [11]. Geletti et al. [10] have highlighted gas seepages, fracture systems, and deep

salt structures based on the interpretation of Sub-bottom chirp profiles. Spatola et al. [11] have shown the acoustic anomalies related to gas occurrence in the Sicily Channel based on the geological interpretation of Sub-bottom profiles, consisting of vertical blanketed areas characterized by acoustically transparent seismic facies.

The acoustic anomalies associated with gas seepage have been observed both within the sediments and at the seabed [12]. Cold seeps are a seafloor expression of the migration of fluids through sediments from the subsurface to the sea bottom and into the water column until they arrive in the atmosphere. They may be generated by microbial activity in the sediments or by thermal processes involving deeper layers. These geological processes mainly ensue on portions of the seafloor, where the expulsion of free and hydrated gas, including methane and other hydrocarbons, occurs. These structures have been recognized globally on active and passive continental margins. On the active continental margins, they have been found in subduction zones and in deltaic environments, where the rapid deposition of sediments and high subsidence have been found. Cold seeps are widespread features of passive continental margins, including the northern US Atlantic Margin. Methane seepage is expected to intensify at these relatively shallow seeps as bottom waters warm and underlying methane hydrates dissociate.

Missiaen et al. [6] have shown seismic evidence of shallow gas. The most evident acoustic anomaly observed on the seismic profiles is acoustic blanking, appearing as diffuse and chaotic seismic facies masking all the other reflections. Acoustic blanking has been observed in the upper sequence and occasionally reaching up to the seabed. Although the acoustic turbidity reaches the surface locally, the sea-floor morphology does not reveal any pockmark.

Andreassen et al. [7] have analyzed shallow gas and fluid migration on the Barents Sea continental margin based on three-dimensional seismic data. The occurrence of gas is inferred from bright spots, while the fluid migration is inferred from vertical zones of acoustic masking and acoustic pipes. The most important indicator of fluid migration is acoustic masking, represented by an area with low seismic reflectivity. It indicates a scattering of the acoustic energy caused by interstitial gas bubbles in the sediments.

The occurrence of gas in Holocene sedimentary successions is of interest both because of shallow-gas accumulations, which may reduce the shear strength of the sediments and pose a hazard to hydrocarbon exploration and development, and because the occurrence of shallow-gas accumulations, and the underlying indications of fluid flow may point towards deeper prospective reservoirs [5,13].

Marine geohazards include fluid flows [13]. Fluid flow through marine sediment is an ordinary process appearing when water from the underlying sediment is removed, when the sediments have been buried and fossilized, biogeochemical processes, hydrothermal activity, or the migration of deep-seated fluid from the acoustic basement. In most cases, fluid accumulates under the sediment when there is rapid sedimentation. Secondary fluids (water and gases) will be added by several geological processes, including the decay of organic matter.

The aim of this paper is to show the occurrence of shallow gas pockets and acoustic anomalies in the inner shelf of the Cilento offshore area based on the geological interpretation of Sub-bottom chirp profiles. A processing sequence has been constructed by reading the seismic sections through Seismic Unix software [14]. Then, this sequence was applied to the seismic record in order to highlight the acoustic anomalies, indicating the occurrence of Quaternary marine deposits enriched by gas. These anomalies include acoustic blanking and the occurrence of wide, acoustically transparent seismic units corresponding to seismic units filled by gas. The location of the study area is shown in Figure 1.

New geologic, seismostratigraphic, and sedimentological data have been recently shown, highlighting the depositional environments in the Cilento offshore are based on marine geological data [15]. An onshore–offshore DEM off the Cilento promontory has been constructed by superimposing the geological results of the marine geological survey at the 1:25.000 scale. Moreover, the geological interpretation of Sub-bottom chirp profiles has

shown the occurrence of shallow gas pockets. However, in a previous paper, the acoustic anomalies related to the occurrence of gas have not yet been discussed in detail; this will be the subject of this paper. Herein, we have improved the quality of previously processed seismic profiles (Seisprho) [16] by assessing a new workflow for the seismic processing of Sub-bottom data with the Seismic Unix software. This has allowed us to improve the previously obtained results on seismic stratigraphy [15] and to focus on the identification of acoustic anomalies related to gas occurrence by constructing new thematic maps in a GIS environment showing the distribution of the shallow gas pockets in the Cilento offshore area.

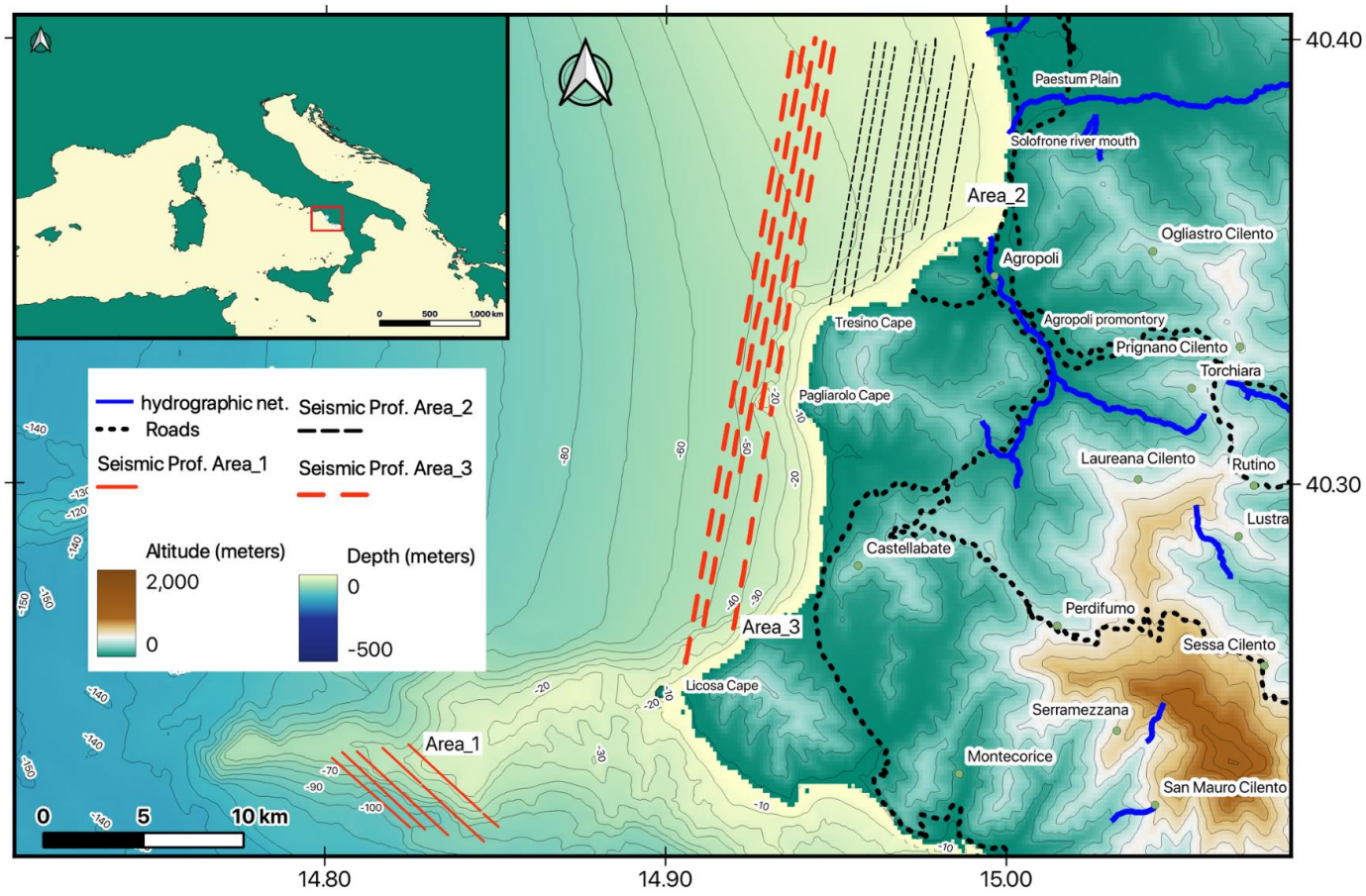

Figure 1. Sketch map showing the location of the seismic profiles analyzed in this paper. Based on the location of the seismic profiles, three main areas have been distinguished, characterized by distinctive acoustic anomalies that are genetically related to the occurrence of gas. The inset on the upper left side shows the general location map of the study area. GIS base was modified after Aiello and Caccavale [15].

Our study will allow us to solve the contrasting hypotheses on the occurrence of shallow gas in the study area, which was not previously singled out based on the bathymetric and geomorphological data recently published on the Cilento offshore area [17]. Violante [17] has carried out a computer-aided geomorphologic seabed classification and habitat mapping of the Punta Licosa Marine Protected Area. The Punta Licosa habitat map shows several marine landforms, including spurs of coralligenous bioconstructions, wave-cut terraces with a mixed organogenic cover, slopes with mixed organogenic sediments, depositional terraces, rocks, deep terraces with bioclastic covers, ledges with coralligenous shelf muddy plains, and sandy fringes with bioclasts and offshore transitions [17]. The pockmarks or other seabed structures that are genetically related to gas occurrence have not been highlighted. Since basic geophysical studies on gas and related seabed

structures have suggested that pockmarks are not necessarily associated with the shallow gas occurring in the subsurface [6,7] (among others), our study will integrate the existing knowledge on shallow gas and the corresponding acoustic anomalies from the offshore Cilento promontory.

2. Geologic Setting

The origin of the sedimentary basins and their subsidence along the Campania sector of the eastern Tyrrhenian margin has been the subject of various studies based on geological field observations and on seismic and well data in the subsurface on land and at sea [18–30]. In this geological context, an important lineament is represented by the 41st parallel line, separating the Northern Tyrrhenian Sea from the Southern Tyrrhenian Sea [31–35].

Along the Campania margin, south of the Aurunci Mountains, the coastal basins are represented by the Garigliano Plain, the Campania Plain, and the Sele Plain. In this sector of the Tyrrhenian margin, the extensional phases were active along the NE-SW trending normal faults, ranging in age from the Late Pliocene to the Quaternary [25,26,36–38]. A chronostratigraphic calibration of the five seismic profiles has been carried out by using data provided by some exploration wells located along the Latium-Campania margin (Michela 1; Mara 1) [25,27].

The continental shelf between the Gulf of Gaeta and the Gulf of Policastro is the seaward prolongation of the alluvial coastal plains (Campania Plain, Sarno Plain, and Sele Plain), bounding the Tyrrhenian sector of the Apennines, which is controlled by high rates of tectonic subsidence [37].

These coastal plains, whose continuity is interrupted by structural highs with a NE-SW trend and by volcanic complexes (Phlegrean Fields and Somma Vesuvius), are limited northeastwards by the inner reliefs of the Apennines. Their sedimentary fill consists of marine and continental clastic deposits, alternating with abundant volcanic products. The acoustic basement is represented by Meso-Cenozoic carbonates ("Campania-Lucania carbonate platform") [39–41] and by Cenozoic-deformed sequences and the related flysch deposits (Cilento Flysch; Sicilide Units; Liguride Units: Figure 2) [42–45].

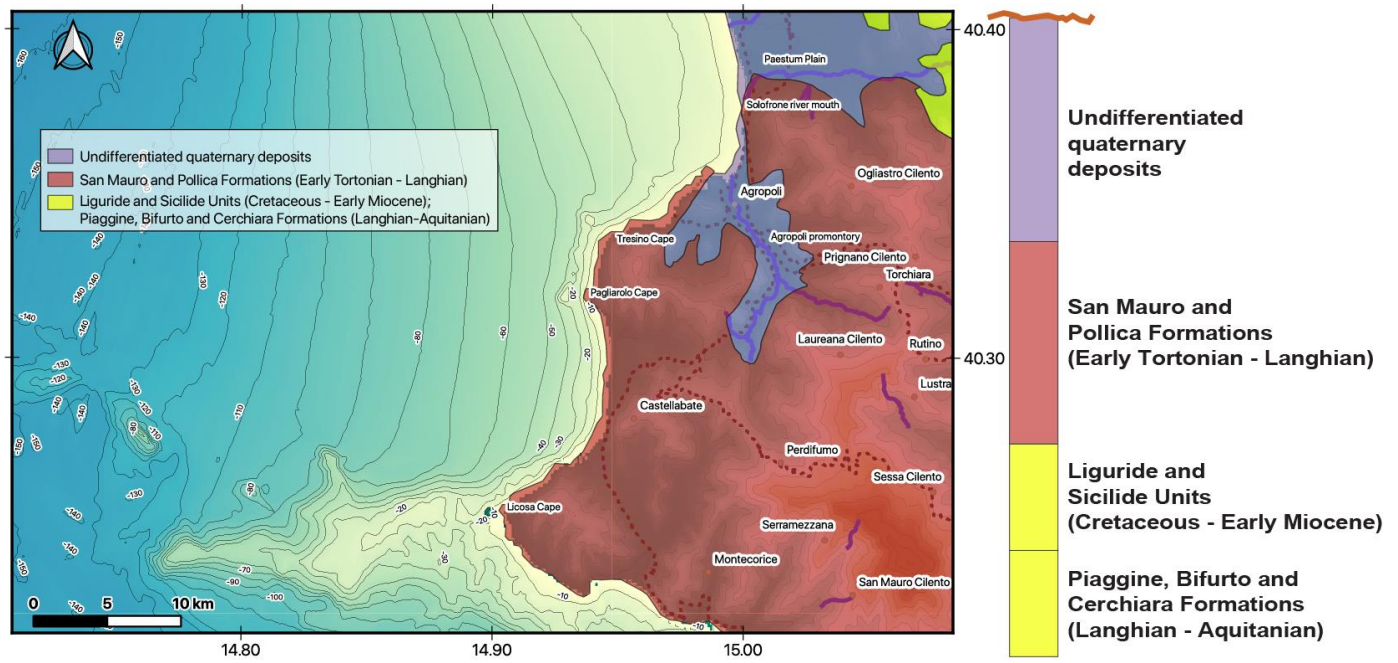

Figure 2. Geologic sketch map of the northern Cilento promontory. Note: the occurrence of main geological units, including the undifferentiated Quaternary deposits, the Cilento Flysch deposits (S. Mauro and Pollica Formations), the Liguride and Sicilide Units, the Trentinara Formation, and the Mesozoic shallow-water limestones. GIS base was modified after Aiello and Caccavale [15].

The Tyrrhenian offshore area between the Sorrento Peninsula and the Cilento promontory, including the half-graben of the Salerno Valley [46,47], is characterized by a wide continental shelf, extending up to 25 km westwards of the Cilento coast, with thin sedimentary cover that becomes thick from a few tens of meters up to a few hundreds of meters.

Southwards of the Sorrento Peninsula, a narrow continental shelf occurs, which is associated with steep slopes, bounding the structural depression of the Salerno Basin. The individuation and the tectonic setting of the Salerno Basin have been mainly controlled by the regional fault Capri-Sorrento Peninsula, with a WSW-ENE trend and an average throw of 1500 m, bounding southwards to the structural high of the Sorrento Peninsula-Capri Island. This fault is composed of several coalescent segments and controls high submarine hazards in the Gulf of Naples [48].

A geological map of the northern Cilento promontory was constructed and imported into a GIS environment (Figure 2).

In this map, several geological units were mapped, including the Quaternary undifferentiated deposits, the S. Mauro and Pollica Formations, which are Langhian–Early Tortonian in age, the Liguride and the Sicilide Units, which are Cretaceous–Early Miocene in age, the Piaggine, Bifurto and Cerchiara Formations, which are Langhian–Aquitanian in age, the Trentinara Formation (limestones and marls), which is Langhian–Aquitanian in age, and the shallow water limestones, which are Late Cretaceous–Liassic in age (Figure 2).

3. Materials and Methods

A scientific theme was developed to carry out the acquisition, processing, and geologic interpretation of a densely spaced grid of high-resolution seismic profiles (Sub-bottom chirp) collected by the CNR-ISMAR onboard the R/V Urania (National Research Council of Italy). The grid of the Sub-bottom chirp seismic sections is reported in Figure 1, which has been constructed in a GIS environment. The chirp linear frequency modulated signals of 2–7 kHz or 8–23 kHz and 4 kW provide high-resolution soundings, reaching up to a 10–30 cm resolution within the uppermost marine sediments, according to the resolution values reported for chirp data by Gasperini and Stanghellini [16]. The obtained data, recorded onboard with a SEG Y format, have been processed by using the software Seismic Unix [14].

The CWP/SU: Seismic Unix is an open-source seismic utilities package that was originally created by the Center for Wave Phenomena at the Colorado School of Mines [14]. This software has been used to convert the seismograms between the SU standard file and the SEG Y files.

Simple processing has been applied to the seismic sections of the Cilento offshore area, consisting of the application of a linear vertical gain along the seismic section, which has allowed for a significant improvement in the quality of the seismic data. The file recorded in the field by the oceanographic cruise was converted from the SEG Y format to the SU format, used by the Seismic Unix software.

The workflow of the processing of the seismic sections consisted of the following steps:

(1) Conversion of the seismic traces from SEG Y to SU;
(2) Spectral analysis of the frequencies of the seismograms, in order to reconstruct the distribution of the frequencies;
(3) Application of fast Fourier transform (FFT) for the visualization and the analysis of the frequencies of the seismic signal. In particular, the Fourier transform converts waveform data in the time domain into the frequency domain. The Fourier transform breaks down the original time-based waveform into a series of sinusoidal terms, each with a single magnitude, frequency, and phase. This process converts a waveform in the time domain that is difficult to describe mathematically into a more manageable series of sinusoidal functions that, when added together, exactly reproduce the original waveform;
(4) Application of a high-pass filter with a low-cut frequency at 150 Hz in order to eliminate the seismic noise and the dark signal. A significant improvement in the

visualization of the seismic reflector of the sea bottom was obtained by using the frequency of 150 Hz;
(5) Application of a uniform gain on each seismic trace;
(6) Application of a time-variant gain (TVG) in order to improve both the seismic signal of the deeper seismic reflectors and the whole visualization of all the seismic profiles;
(7) Output of the seismic profiles with Seismic Unix in order to obtain the final files, which were plotted using a graphic interface.

The geological interpretation of the Sub-bottom chirp data was carried out based on the seismostratigraphic criteria [49–51]. The basic principle of seismic stratigraphy is that the seismic reflectors, determined by the contrasts of acoustic impedance, correspond to the strata plans. Perhaps, the geometry of the seismic reflectors corresponds to the depositional geometry. The contrasts of acoustic impedance, which are the product of the seismic velocity for the density of the crossed grounds, control the location of the seismic reflectors and are located along the strata surfaces or other discontinuities, having a chronostratigraphic meaning. The strata surfaces represent the old depositional surfaces and perhaps are coeval in the depositional area.

The discontinuities are old erosional or nondepositional surfaces, corresponding with significant stratigraphic gaps. Even though they represent events that vary over geological time, the discontinuities are chronostratigraphic surfaces because the layers overlying the discontinuity are younger than the underlying layers [49–51].

4. Results

The study area represents a wide continental shelf, for which the outer margin is located at a water depth of 250 m. While the continental shelf northwards of the Licosa Cape has uniform gradients, the marine area surrounding the Licosa Cape represents an E–W trending structural high, characterized by the remnants of the terraced surfaces, which erode the rocky basement. A break in slope at water depths ranging from 60–80 m marks the passage from the structural high of the Licosa Cape to the outer shelf through a steep slope. Towards the Policastro Gulf, the continental slope is characterized by an articulated morphology and high gradients at water depths ranging from 10–110 m [15] (Figure 3).

The relict morphologies that are NNW-SSE to E-W trending occur both northwestwards and southwestwards of the Licosa Cape and are genetically related to the Middle-Late Pleistocene continental shelf [15] (Figure 3). The palimpsest deposits are of an emerged–submerged beach form of elongated dunes, composed of well-sorted sands and gravels that are often cemented, with abundant bioclastic fragments that are sometimes overlain by thin drapes of bioclastic sands of the outer shelf. On the Sub-bottom chirp lines, the relict sands appear as deaf units with slightly inclined clinoforms, with offsets truncated at the sea bottom by polycyclic erosional surfaces [15].

The sedimentological analyses show the grain-size distribution of the sediments on the seafloor, including sandy gravels, gravelly sands, sands, silty sands, muddy sands, sandy silts, silts, and muds [15]. Ternary plots of the sea bottom samples were constructed (shales-sands-silts and gravels-sands-silts) in order to improve the processing of the sedimentological data. Fine-grained sands are widespread along the coast in the northern region and in the offshore area of the Licosa Cape. Coarse-grained sands are located in the offshore area of the Licosa Cape.

A sketch of a morphobathymetric map and a geologic map was constructed in a GIS environment, aimed at showing the main morphostructural features of the studied area (Figure 3) [15]. The main geomorphological features are represented by channels, abrasion terraces, an acoustic substratum, and sandy bodies. Important channels start from the 20 m isobaths on the inner shelf from the Pagliarolo Cape towards the Licosa Cape, while other channels start from the outcrops of the acoustic substratum surrounding the Licosa Cape (Figure 3) [15]. A wide outcrop of the acoustic basement that is elongated in shape and E–W trending is located offshore to the Licosa Cape promontory, reaching water depths exceeding 100 m (Figure 3). Northeastwards of the main outcrop, two minor outcrops occur

that are, respectively, NE-SW and NW-SE trending (Figure 3) [15]. Otherwise, southwards, another outcrop has been detected (Figure 3). For a detailed description of the Quaternary marine deposits, refer to the paper of Aiello and Caccavale [15].

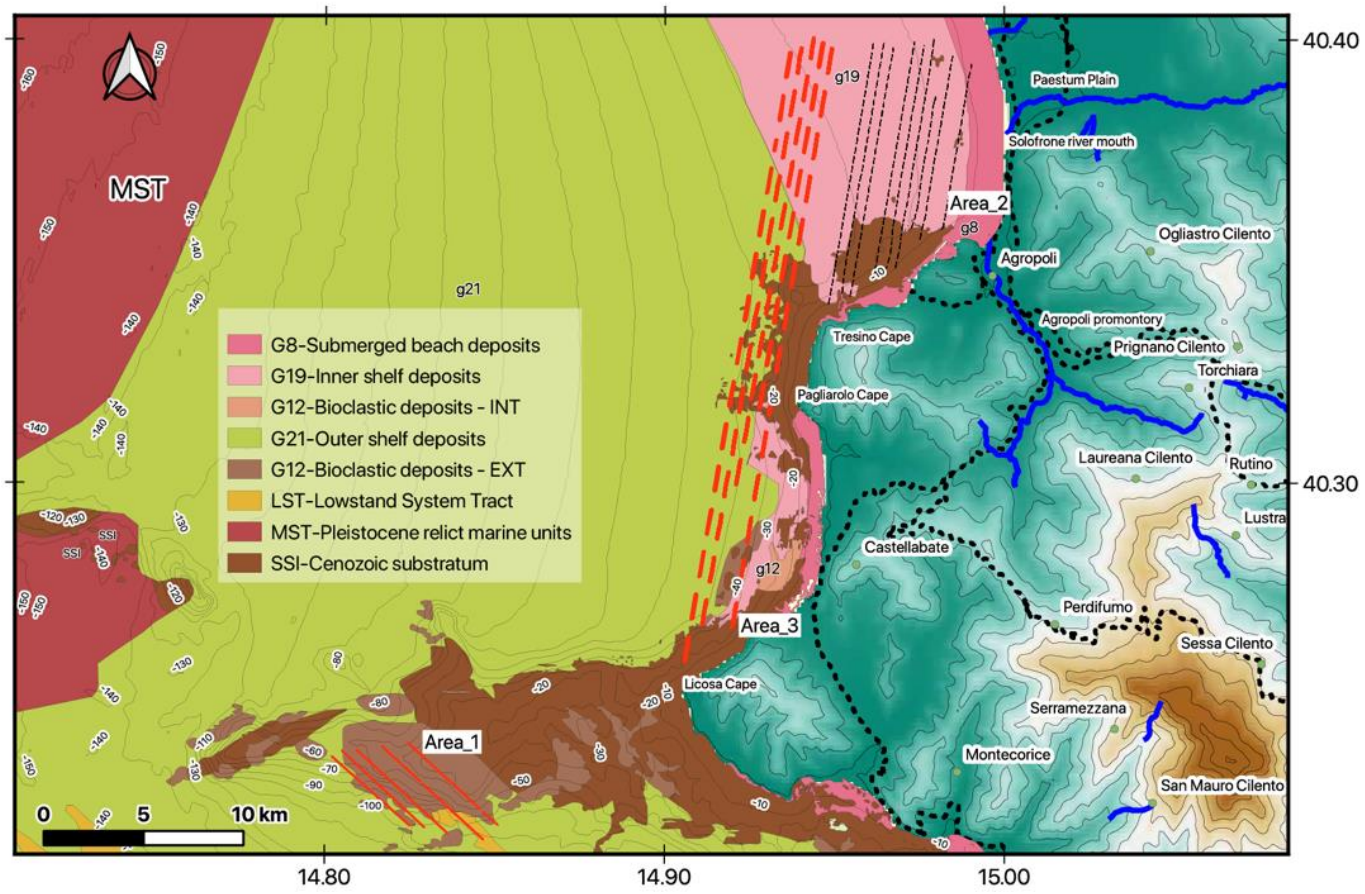

Figure 3. Sketch of a morphobathymetric and geologic map of the analyzed area. The main geomorphological lineaments occurring in this area have been reported, coupled with Quaternary marine deposits (modified after [15]).

Three areas were distinguished based on seismic interpretation in order to highlight the different acoustic features recognized in the Cilento offshore area (Figures 1 and 3).

A sketch table has been constructed in order to improve the understanding of the areas involved by gas and other corresponding acoustic features (Table 1).

Based on the identified features, the first area is located offshore from the Licosa Cape promontory at water depths ranging between 30 and 90 m (Figure 1). It is composed of seven seismic sections (B33_1, B33a_1, B35_1, B35a_1, B37_1, B38, and B39), whose distinctive acoustic features are represented by acoustic blanking, controlled by the occurrence of gas. The wide occurrence of rocky acoustic basements composed of the ssi unit corresponding with the seaward prolongation of the Cilento Flysch, widely cropping out in the adjacent coastal sector, can be singled out. In fact, the seismic lines appear to be located on the flank of a wide outcrop of the rocky acoustic basement, distinguishing the offshore sector (Figure 3) [15].

Table 1. Sketch table showing the areas of the acoustic features, the corresponding seismic sections and the related shot points, and the acoustic features recognized based on seismic interpretation.

	Seismic Sections	Shot Points	Acoustic Features
1	B33_1	400–550; 800–1100; 1450–1750	acoustic blanking
1	B33a_1	350–490	acoustic blanking
1	B35_1	1250–1400 1900–2100 2350–3100	acoustic blanking
1	B35a_1	0–380 750–900 1600–1850 2600–2800 3200–3400	acoustic blanking
1	B37_1	1000 2500 3500–4000	acoustic blanking
1	B38	700–800 1200–1500 2300–2500 3200–3600 4550–5100	acoustic blanking
1	B39	100–500 700–750 1100–1400 2400–2550 3100–3400 3900–4000 4400–4600 5000–5400	acoustic blanking
2	B43	2900–3200	shallow gas pockets
2	B45		no feature
2	B46		no feature
2	B47		no feature
2	B48		no feature
2	B49	2000–2500	shallow gas pockets
2	B51	0–0.1 ($\times 10^4$)	shallow gas pockets
2	B52	0–0.18 ($\times 10^4$) 0.25–0.45 ($\times 10^4$) 0.7–0.85 ($\times 10^4$)	seismic units impregnated of gas
2	B53	0.4–0.7 ($\times 10^4$) 0.75–1.1 ($\times 10^4$)	seismic units impregnated gas
3	B61	0.3–0.45 ($\times 10^4$) 0.45–1.2 ($\times 10^4$)	seismic units impregnated gas
3	B62a	1.15–1.2 ($\times 10^4$) 1.3–1.45 ($\times 10^4$)	shallow gas pockets
3	B63	0.1–0.48 ($\times 10^4$) 0.55–0.7 ($\times 10^4$)	seismic units impregnated gas

Table 1. *Cont.*

	Seismic Sections	Shot Points	Acoustic Features
3	B64	0.2–0.5 ($\times 10^4$) 0.5–0.7 ($\times 10^4$)	shallow gas pockets seismic units impregnated gas
3	B65	180–400 500 600–800	shallow gas pockets
3	B65_1	0–0.8 ($\times 10^4$)	seismic units impregnated gas

The second area is, instead, located in the northern Cilento promontory from the seaward prolongation of the Paestum Plain, proceeding southwards up to the Tresino Cape (Figure 1). It is composed of nine seismic sections (B43, B45, B46, B47, B48, B49, B51, B52, and B53), whose distinctive acoustic features are represented by shallow gas pockets (Table 1). The seismic sections have highlighted the occurrence of thick sedimentary cover, organized in several seismostratigraphic units, mainly Holocene in age [15].

The third area is located on the northern Cilento promontory, starting from the offshore prolongation of the Paestum Plain up to the Licosa Cape promontory, at water depths ranging between 10 and 60 m (Figure 1). It is composed of six seismic sections (B61, B62a, B63, B64, B65, and B65_1; Table 1), whose distinctive features are represented by shallow gas pockets and by the seismic units impregnated by gas ("gassy sediments").

A seismic analysis of the Sub-bottom chirp profiles has allowed us to study the seismostratigraphic characteristics of the Cilento offshore area between the Solofrone River mouth and the Licosa Cape. The main outcrops at the sea bottom of the rocky acoustic basement have been bounded relative to the sedimentary covers, which are composed of coarse-grained sands, grading towards middle-fine-grained sands and fine-grained sands. The sandy facies are prevalent in the sector of the continental shelf located between the Solofrone River mouth and Agropoli, where they form a wide system of coarse-grained sandy belts with an N–S trend parallel to the isobaths and are located at water depths ranging between 10 m and 17 m. In the same area, the rocky outcrops have a limited extension and occur at water depths ranging between 15 m and 20 m.

The rocky acoustic basement (ssi) widely crops out next to the shoreline from Agropoli to the Tresino Cape and from the Tresino Cape to the Pagliarolo Cape (Figure 3), where it represents the seaward prolongation of the coastal cliffs incised in the deposits of the Cilento Flysch [41,43,45].

The seismic lines B51, B52, and B53 have been taken as an example among the existing seismic lines in order to highlight the occurrence of wide shallow gas pockets and to show the significant improvement in the seismic lines obtained by introducing the Seismic Unix processing with respect to the processing carried out with the Seisprho [15].

In the northern Cilento offshore area, between the Solofrone River mouth and the Licosa Cape, the seismostratigraphic analysis showed that the recent sedimentary cover, ranging in age between the Late Pleistocene and the Holocene, is organized into three main seismostratigraphic units, overlying the undifferentiated acoustic basement (ssi).

The seismic interpretation (Figure 4) shows that the first unit (seismostratigraphic unit 1) is characterized by acoustically transparent seismic facies and ranges in thickness between 7 m and 10 m. Unit 1, probably composed of sands, unconformably overlies the undifferentiated acoustic basement (ssi). Its top is strongly eroded, forming palaeochannels in which the seismostratigraphic unit 2 was deposited.

The second unit (seismostratigraphic unit 2; Figure 4) is distinguished from alternating acoustically transparent intervals and continuous intervals, probably corresponding with alternating sands and shales, for a whole thickness of about 10 m. The unit forms the

filling of the palaeochannels individuated at the top of unit 1 and the erosional depressions located at the top of the ssi substratum.

The third unit (seismostratigraphic unit 3; Figure 4) is characterized by acoustic facies with parallel and discontinuous reflectors of high amplitude, and represents the recent filling, Holocene in age.

The seismostratigraphic setting of the first area, as shown in Table 1 and in Figure 4, is exemplified by the seismic interpretation of the seismic sections shown in Figures 5–7.

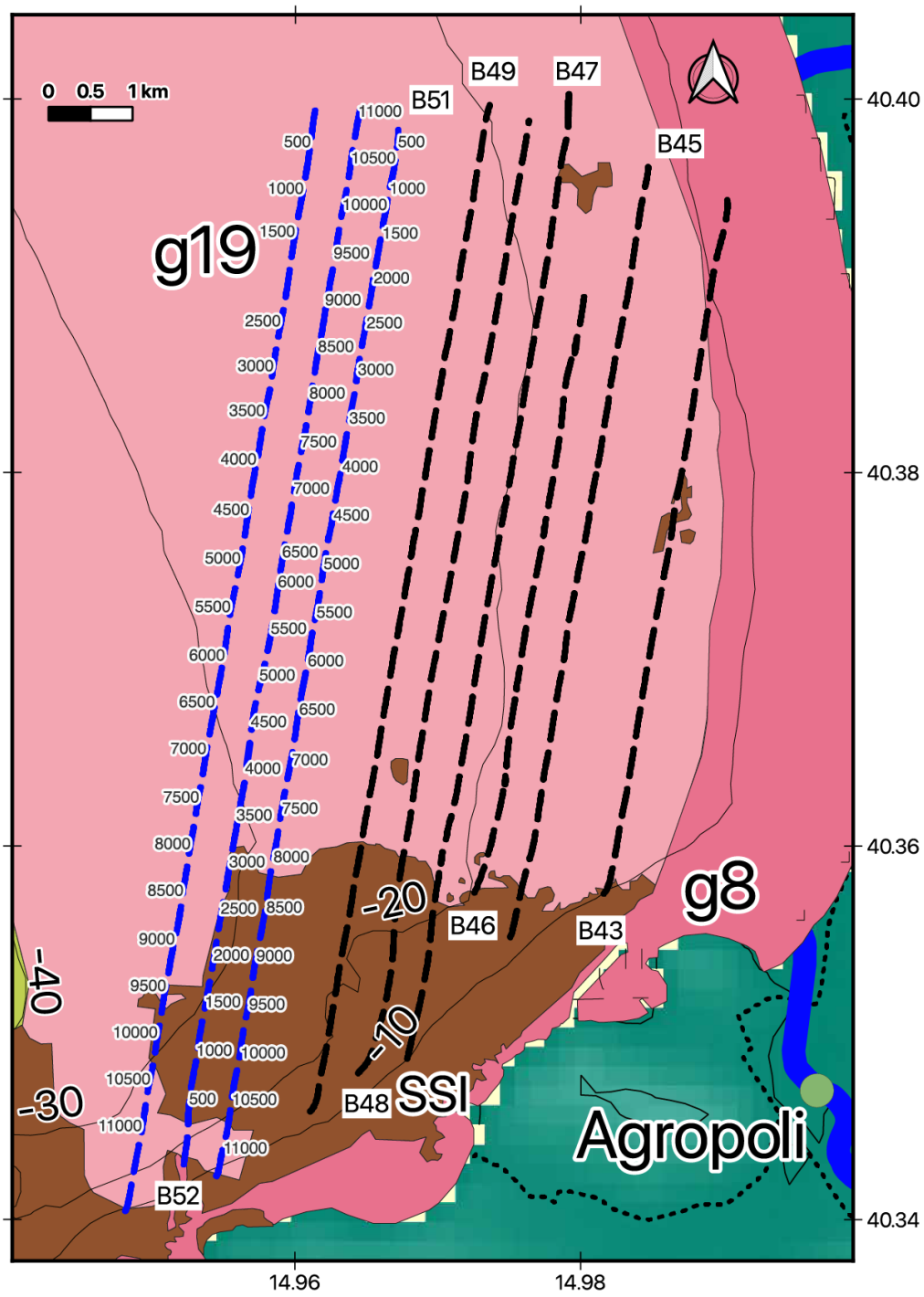

Figure 4. *Cont.*

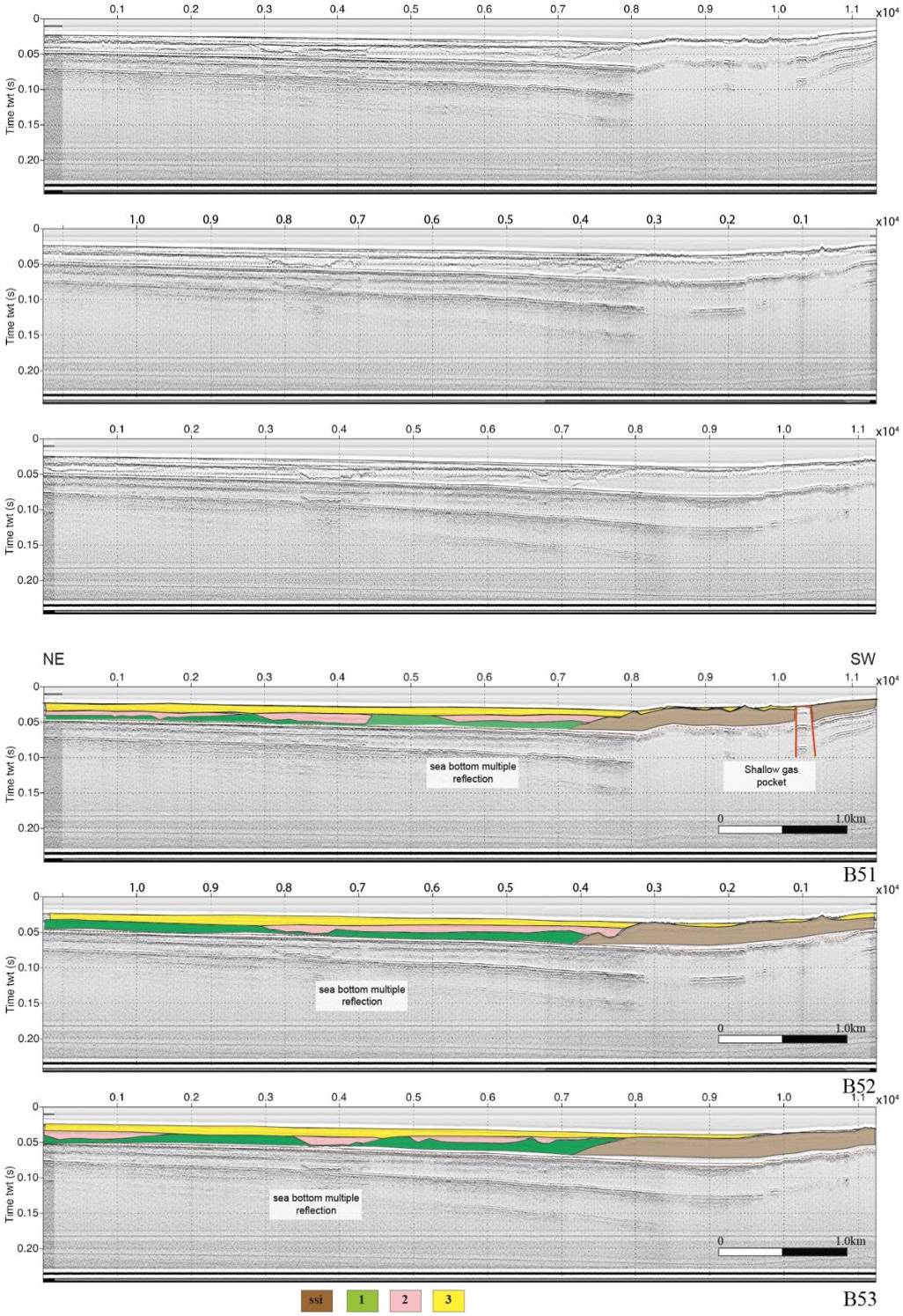

Figure 4. (**top**) Sketch location map of the Sub-bottom chirp profiles; (**middle**) Sub-bottom chirp profiles B51, B52, and B53 and (**bottom**) corresponding geologic interpretation. Note the occurrence of the three main seismostratigraphic units (1, 2, 3) overlying the undifferentiated acoustic basement (ssi; see the text for further description).

The seismic profile B33_1 crosses a wide outcrop of the acoustic basement (ssi unit), which is genetically related to the Cilento Flysch (Figure 5). On the north-western side of the seismic section, three wide areas of acoustic blanking have been identified, suggesting the occurrence of gas impregnations (Figure 5). The seismic profile B33a_1 (area 1) has shown

the wide outcrop of the acoustic basement (ssi unit), overlain by a recent sedimentary cover (Figure 5). The interpretation of the seismic section has suggested the occurrence of a wide area of acoustic blanking between the shot points 350 and 480, highlighting the occurrence of gas impregnations (Figure 5).

The seismic profiles B35_1 and B35a_1 show a similar stratigraphic setting, with wide outcrops for the acoustic basement (ssi unit), overlain by the recent sedimentary cover (Figure 6). The interpretation of the seismic sections has shown the occurrence of several areas of acoustic blanking (Table 1) with gas impregnations.

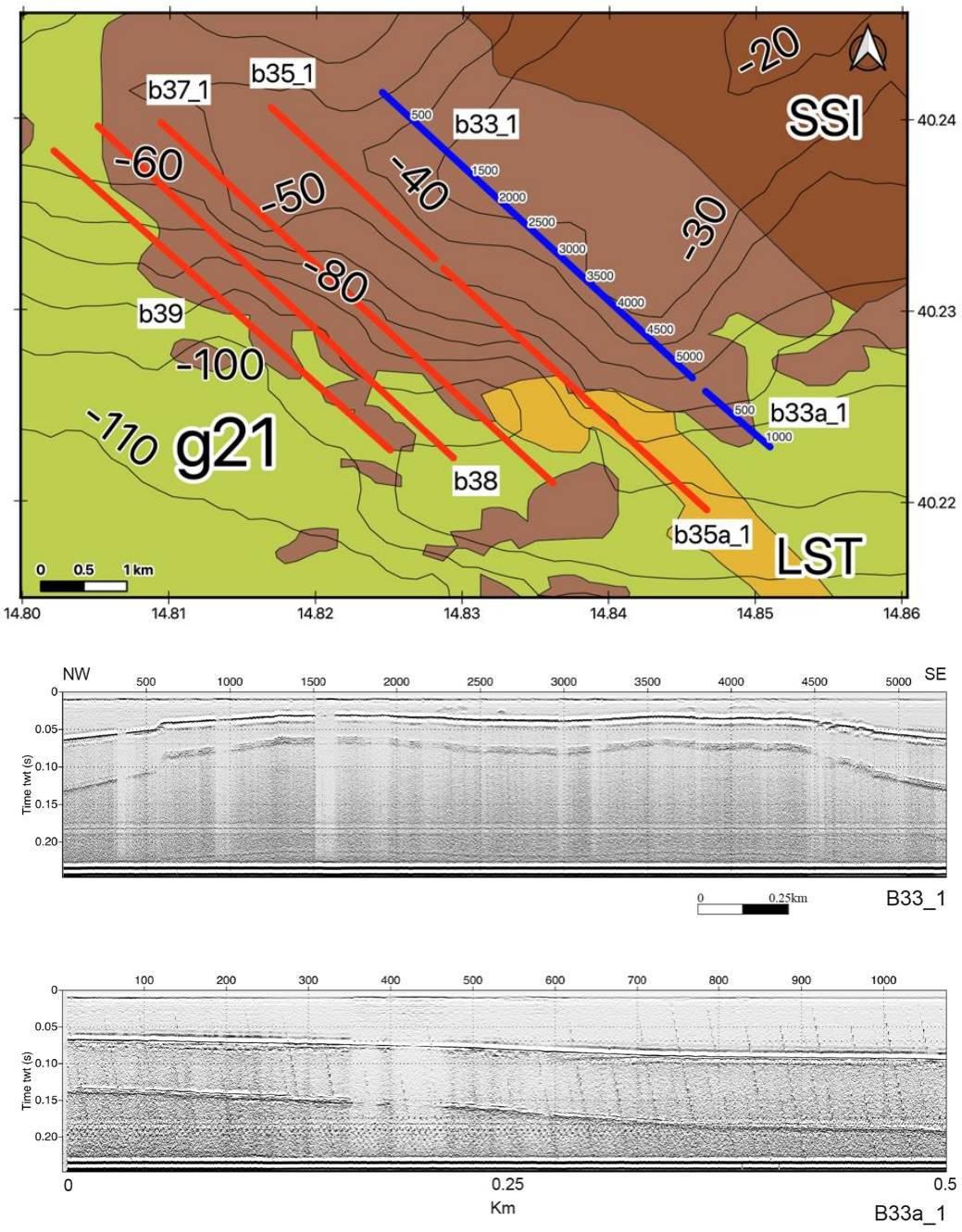

Figure 5. *Cont.*

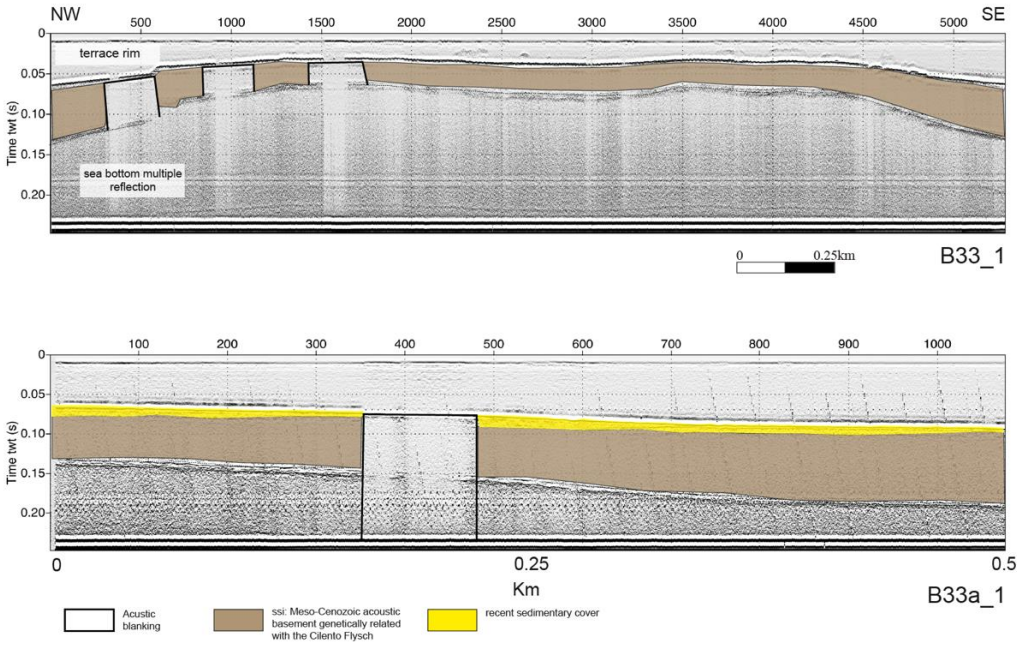

Figure 5. (**top**) Sketch location map of the Sub-bottom chirp profiles of area 1; (**middle**) Sub-bottom chirp profiles B33_1 and B33a_1 and corresponding geologic interpretation (**bottom**).

The seismic profiles B37_1, B38, and B39 show wide areas of acoustic basement (ssi unit) overlain by a thin recent sedimentary cover. All three seismic sections have highlighted the occurrence of shallow gas pockets, as shown by the seismic interpretation (Figure 7).

The seismic profiles B43 and B45 (area 2: Figure 8-top) show a stratigraphic setting characterized by three main seismostratigraphic units, corresponding with Holocene marine deposits, Holocene coastal and marine sands, and coastal sands, which are Late Holocene in age (Figure 8-middle). On the seismic profile B43, a wide shallow gas pocket was identified (Figure 8-middle).

The seismic profile B46 shows three main seismostratigraphic units, respectively, corresponding to the Holocene marine deposits, with coastal and marine sands that are Holocene in age, and coastal sands, which are Late Holocene in age (Figure 9). The coastal and marine sands are interpreted as a wide seismic unit of gassy sediments due to their seismic facies. The interpretation of the seismic profile B47 shows the occurrence of four main seismostratigraphic units, respectively corresponding with the ssi unit, interpreted as the Meso-Cenozoic acoustic basement that is genetically related to the Cilento Flysch, with the marine deposits (Holocene in age), and with the coastal sands. The coastal sands represent the filling of a wide palaeodepression since they thicken toward the center of the depression and thin toward both the sides (Figure 9).

The seismic profiles B48 and B49 (Figure 10) show the occurrence of five main seismostratigraphic units, respectively, represented by the ssi unit (Meso–Cenozoic acoustic basement, genetically related with the Cilento Flysch), marine deposits, the coastal and marine sands (both Holocene in age), a seismic sequence filling the palaeochannels, and by the coastal sands (Late Holocene in age) (Figure 10).

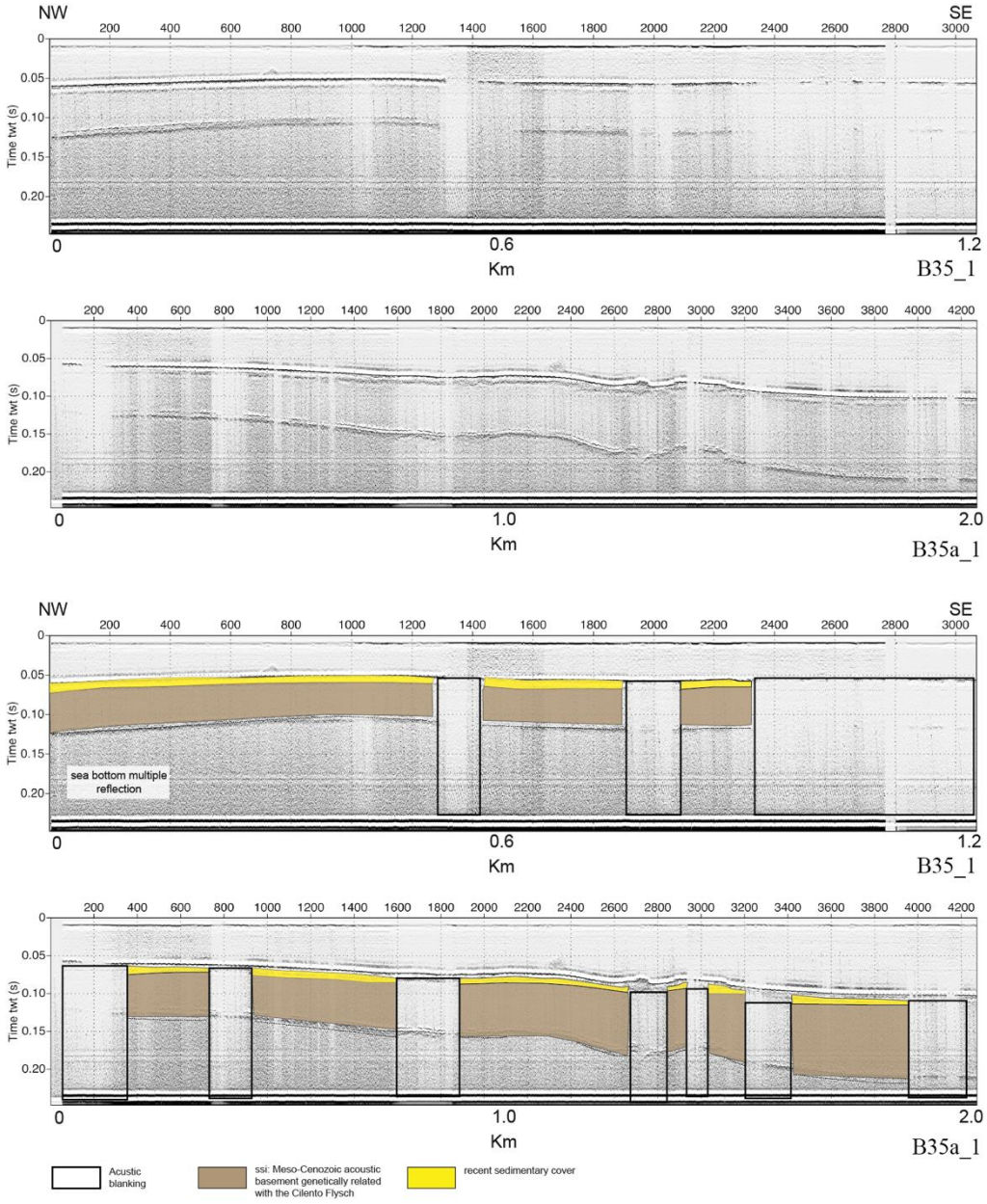

Figure 6. (**top**) Sketch location map of the Sub-bottom chirp profiles of area 1; (**middle**) Sub-bottom chirp profiles B35_1 and B35a_1 and the corresponding geologic interpretation (**bottom**).

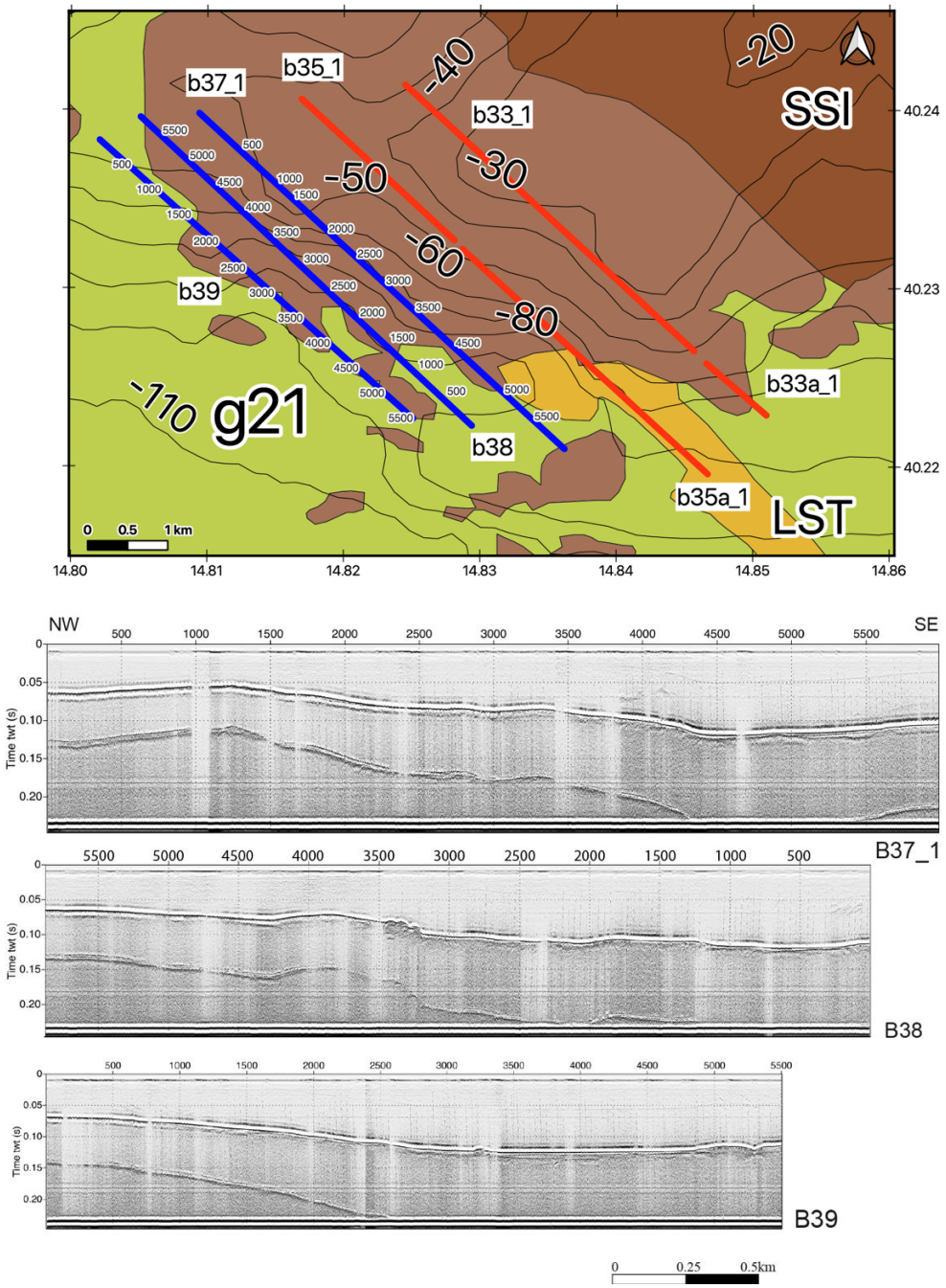

Figure 7. *Cont.*

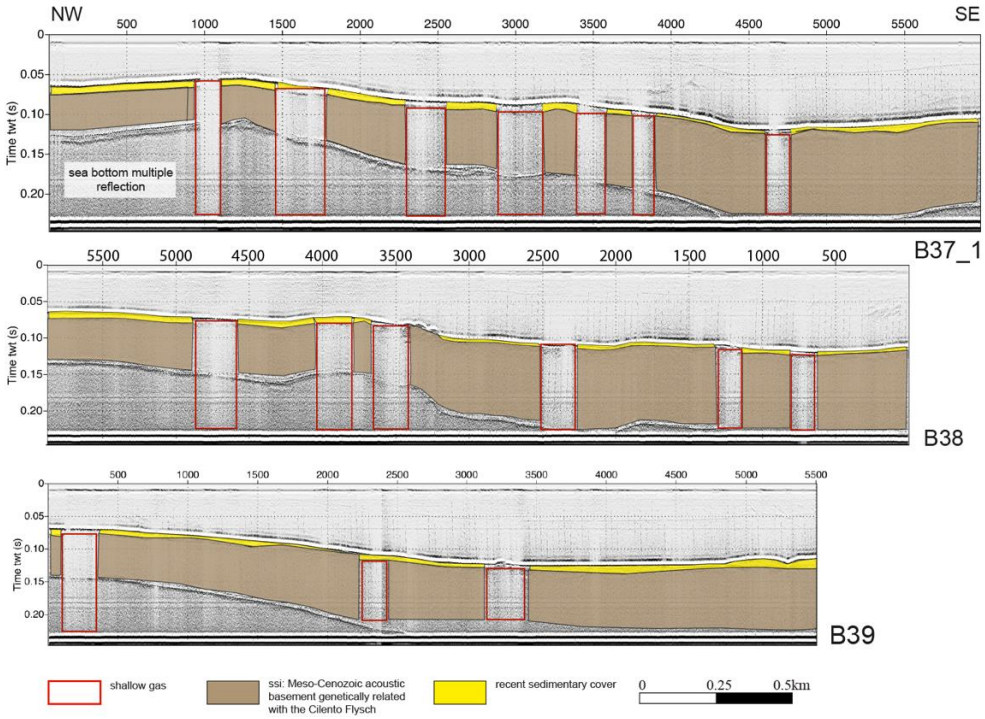

Figure 7. (**top**) Detailed location map; (**middle**) Sub-bottom chirp profiles B37_1, B38, and B39 and the corresponding geologic interpretation (**bottom**).

The seismic profiles B61 and B62_a show the occurrence of five main seismostratigraphic units (Figure 11). The ssi unit constitutes a small morphostructural high occurring in the central part of the seismic section from the shot point 1.2 to 1.8. Proceeding onshore, this seismic unit prolongates on the side of the morphostructural high, below the seismo-stratigraphic unit of the coastal and marine sands, representing gassy sediments below the coastal sands (Late Holocene in age). On the seismic profile B62_a, the same unit composes a small outcrop. The coastal and marine sands (Holocene in age) represent a wide, acoustically transparent seismic unit, interpreted as gassy sediments (Figure 11). Moreover, the coralligenous deposits are interpreted as facies hetheropy with coastal sands (Holocene in age) (Figure 11).

The seismic profiles B63 and B64 show the wide seismostratigraphic units of coastal sands, interpreted as gassy sediments, seismostratigraphic units for channel filling, and seismostratigraphic units for coralligenous deposits in facies hetheropy with coastal sands (Figure 12).

The seismic profiles B65 and B65_1 show the seismostratigraphic units of coastal and marine sands (Holocene in age) overlain by coastal sands (Late Holocene in age) (Figure 13). Two wide areas of acoustic blanking were detected at the shot points between 200 and 800 (Table 1). Moreover, the seismic profile B65_1 shows wide outcrops of acoustic basement (ssi unit). The seismostratigraphic units of channel filling are characterized by disrupted seismic reflectors controlled by the occurrence of gas (Figure 13).

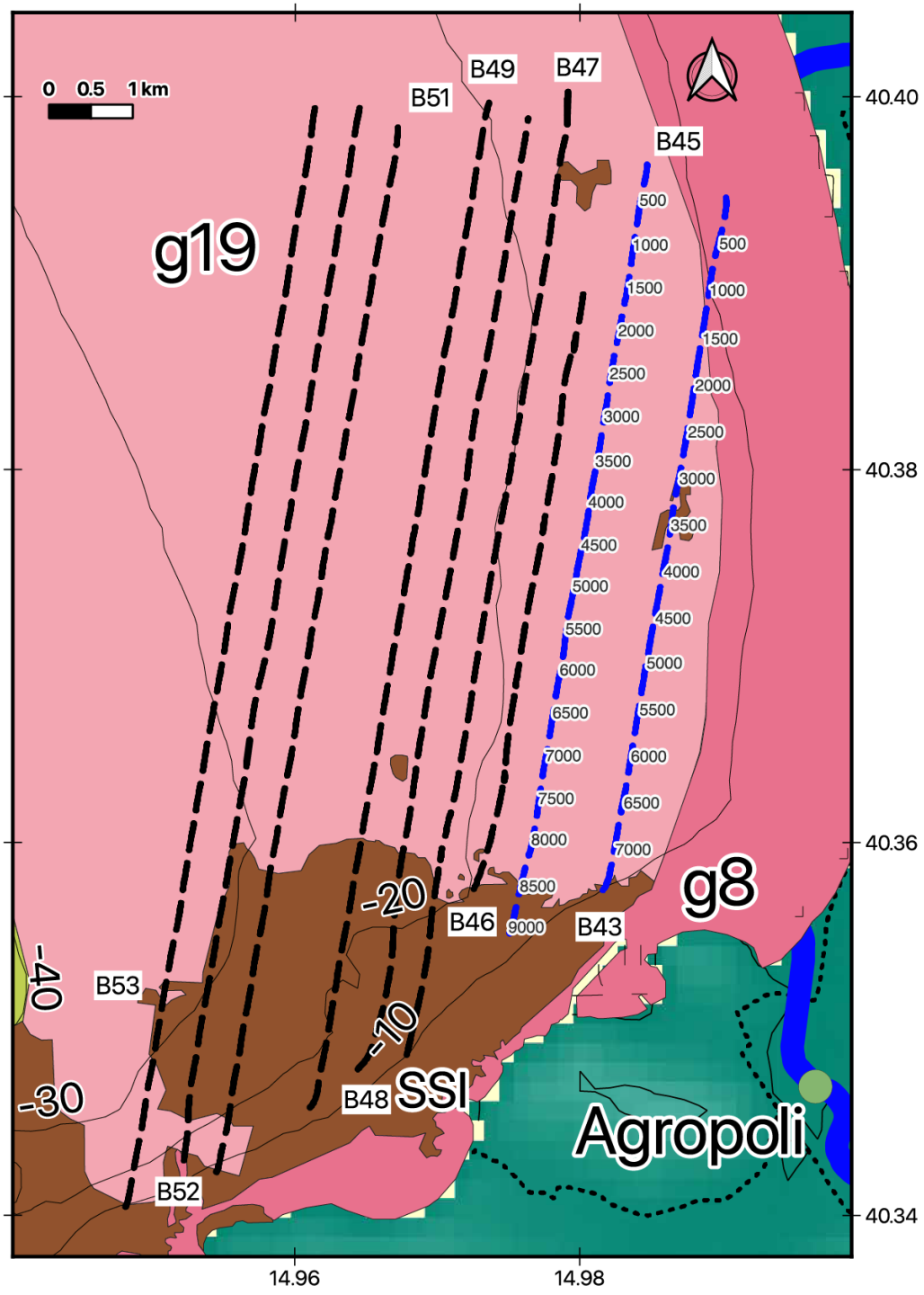

Figure 8. *Cont.*

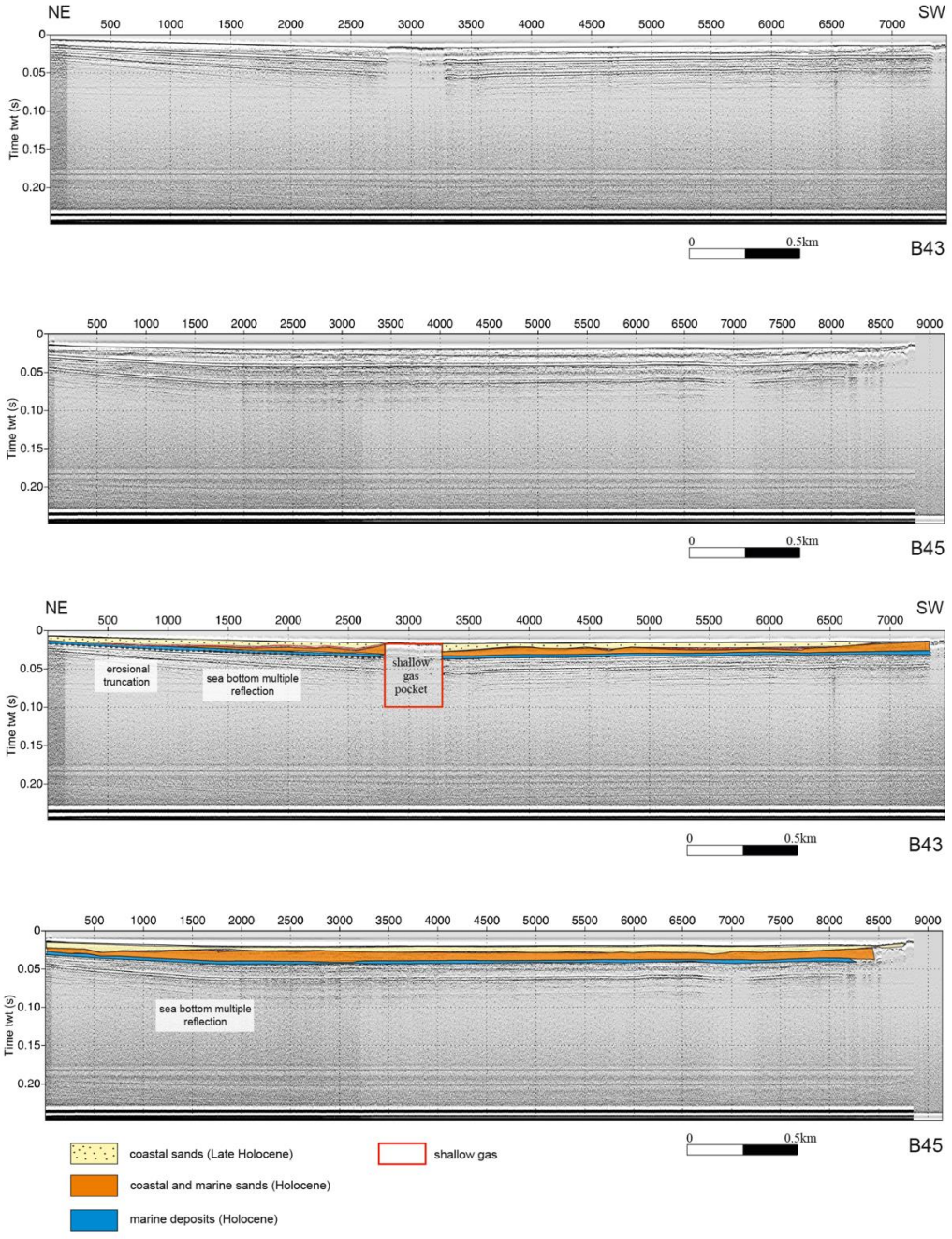

Figure 8. (**top**) Sketch location map of the Sub-bottom chirp profiles of area 2; (**middle**) Sub-bottom chirp profiles B43 and B45 and the corresponding geologic interpretation (**bottom**).

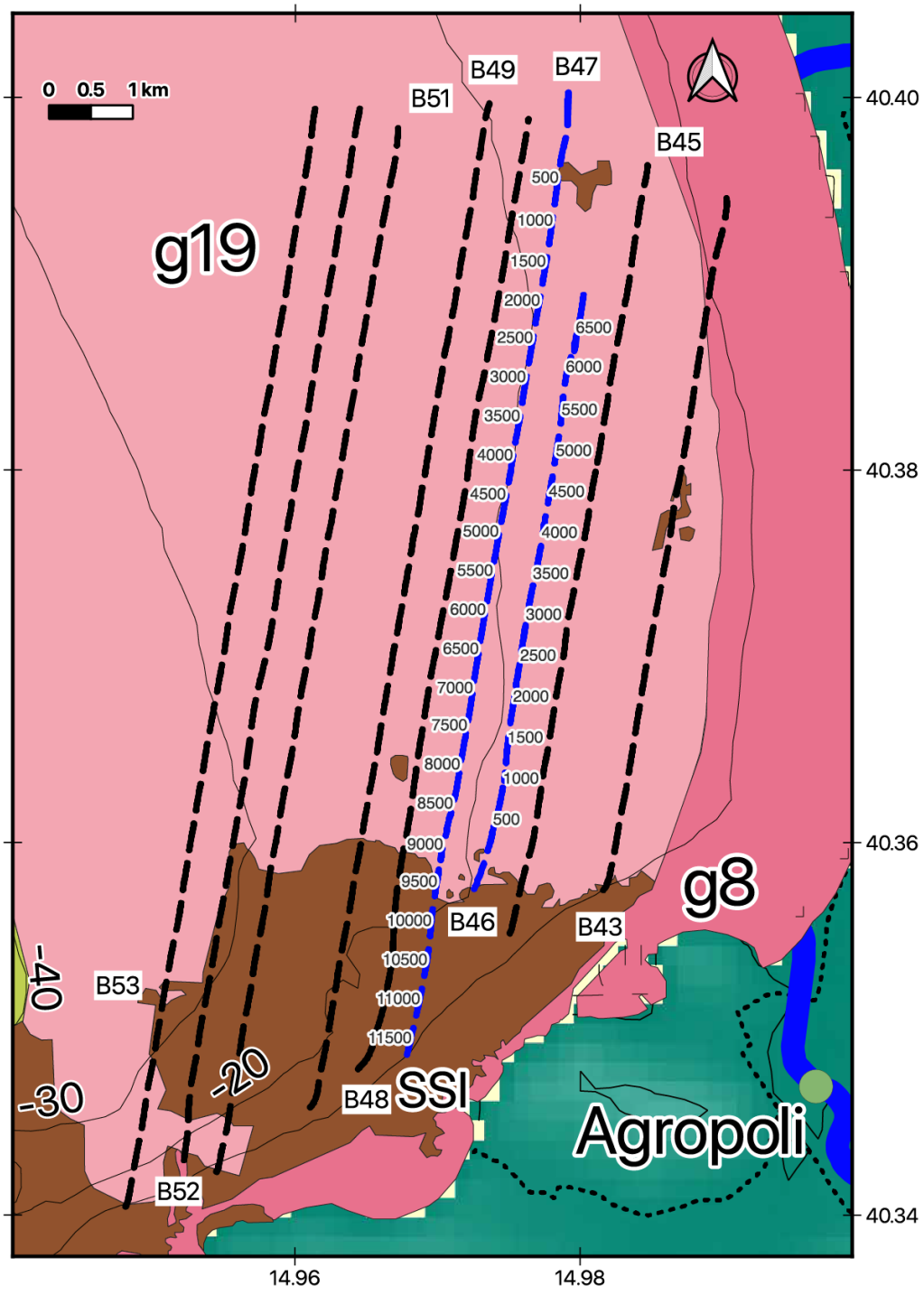

Figure 9. *Cont.*

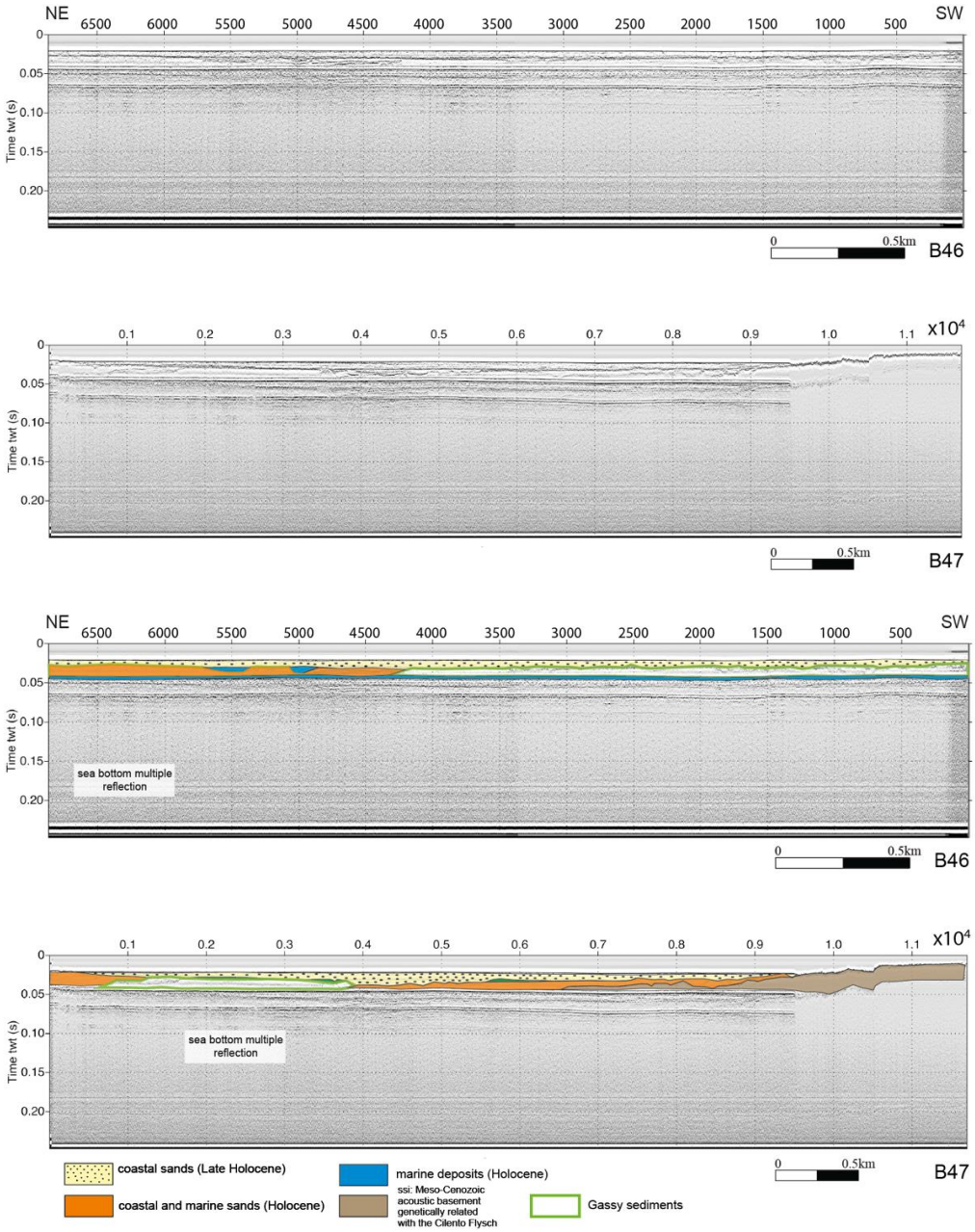

Figure 9. (**top**) Detailed location map; (**middle**) Sub-bottom chirp profiles B46 and B47 and the corresponding geologic interpretation (**bottom**).

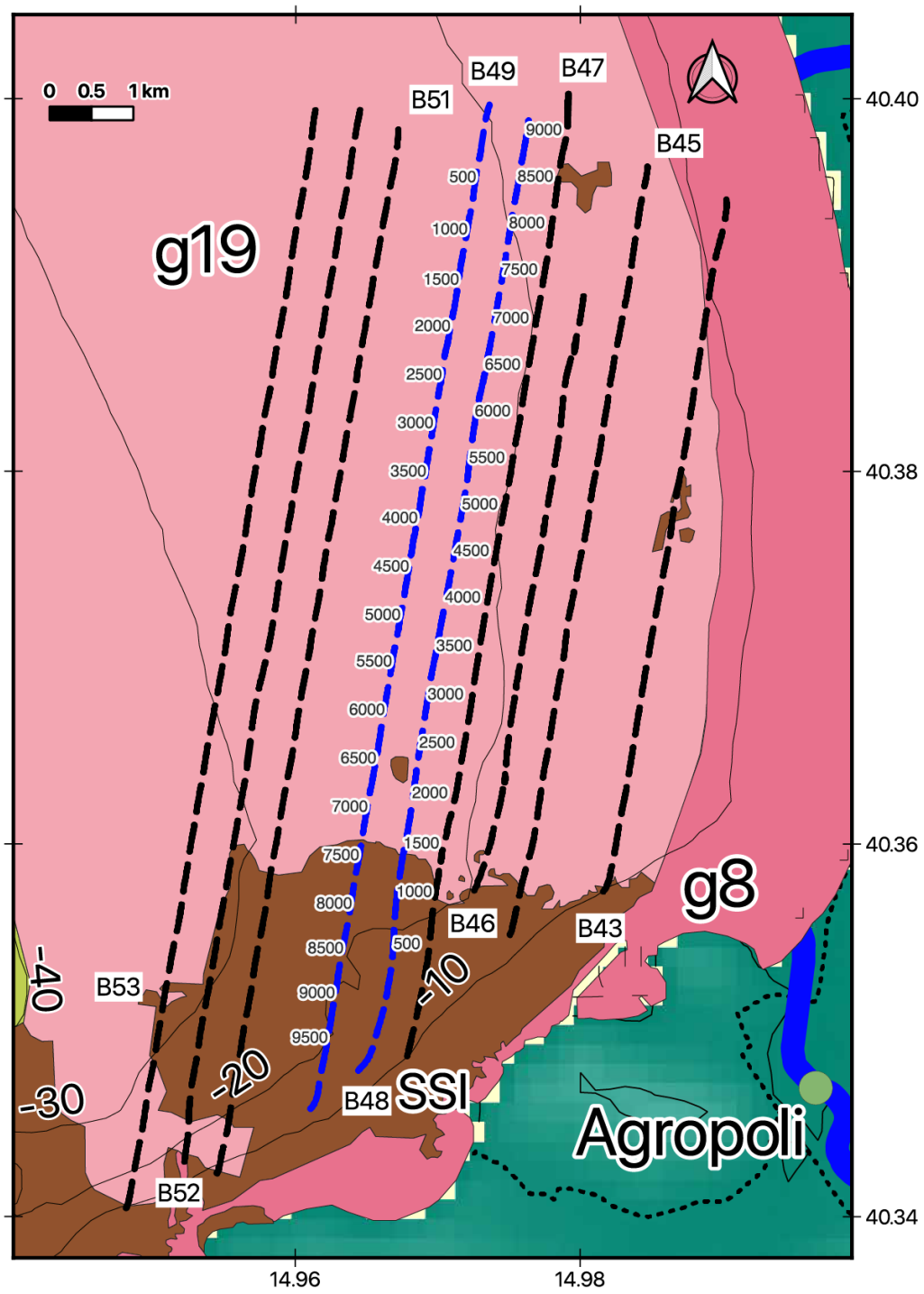

Figure 10. *Cont.*

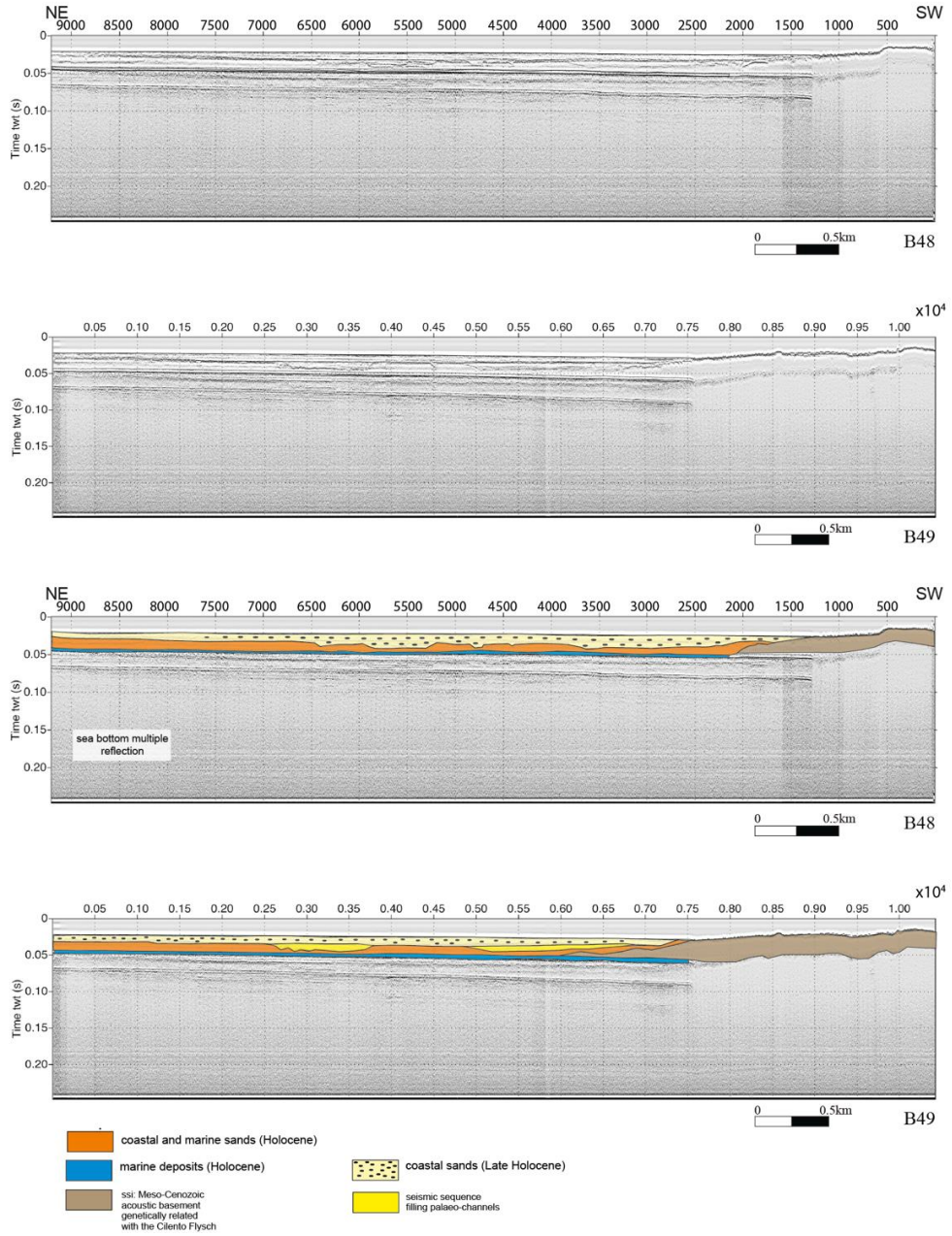

Figure 10. (**top**) Detailed location map; (**middle**) Sub-bottom chirp profiles B48 and B49 and the corresponding geologic interpretation (**bottom**).

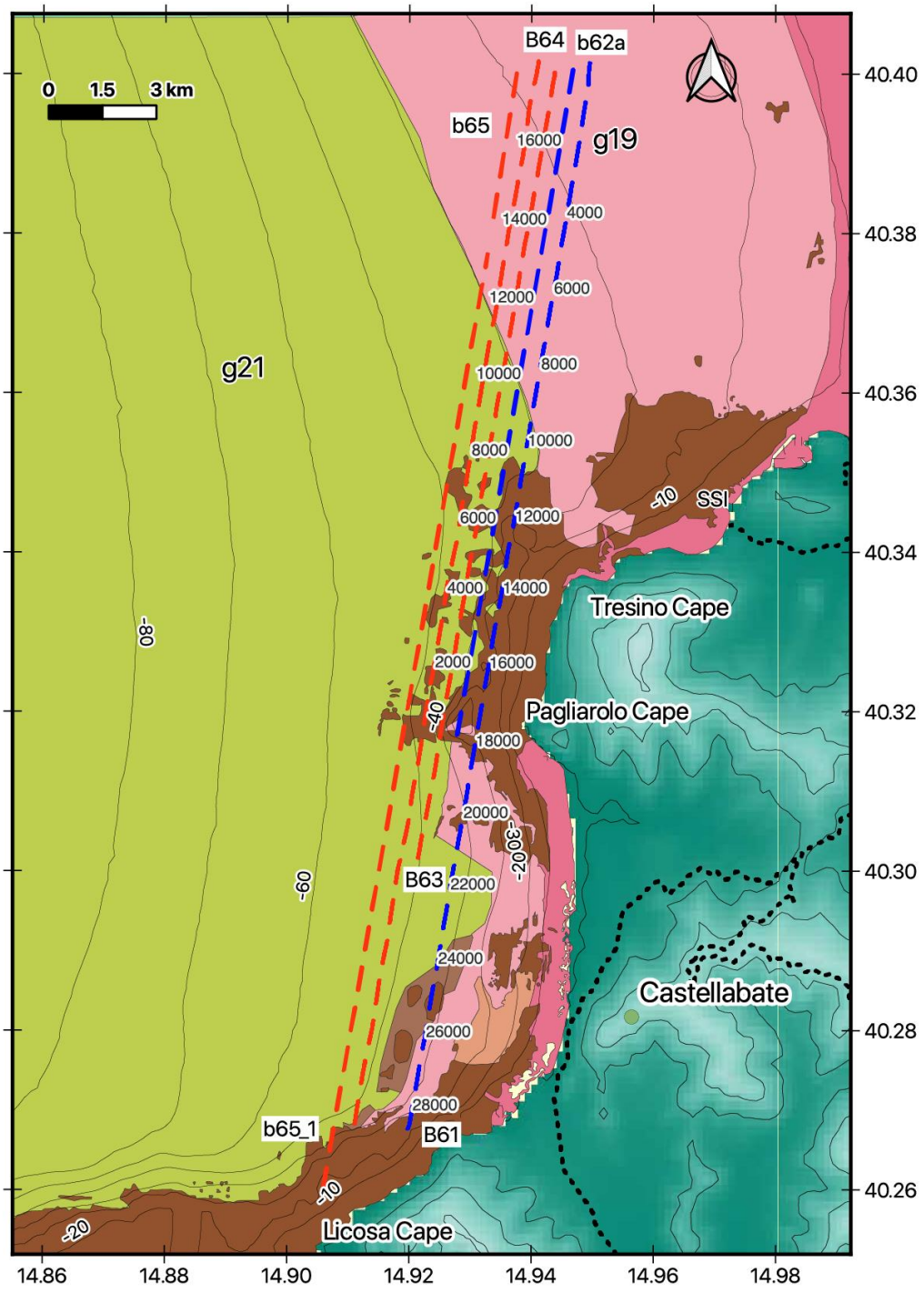

Figure 11. *Cont.*

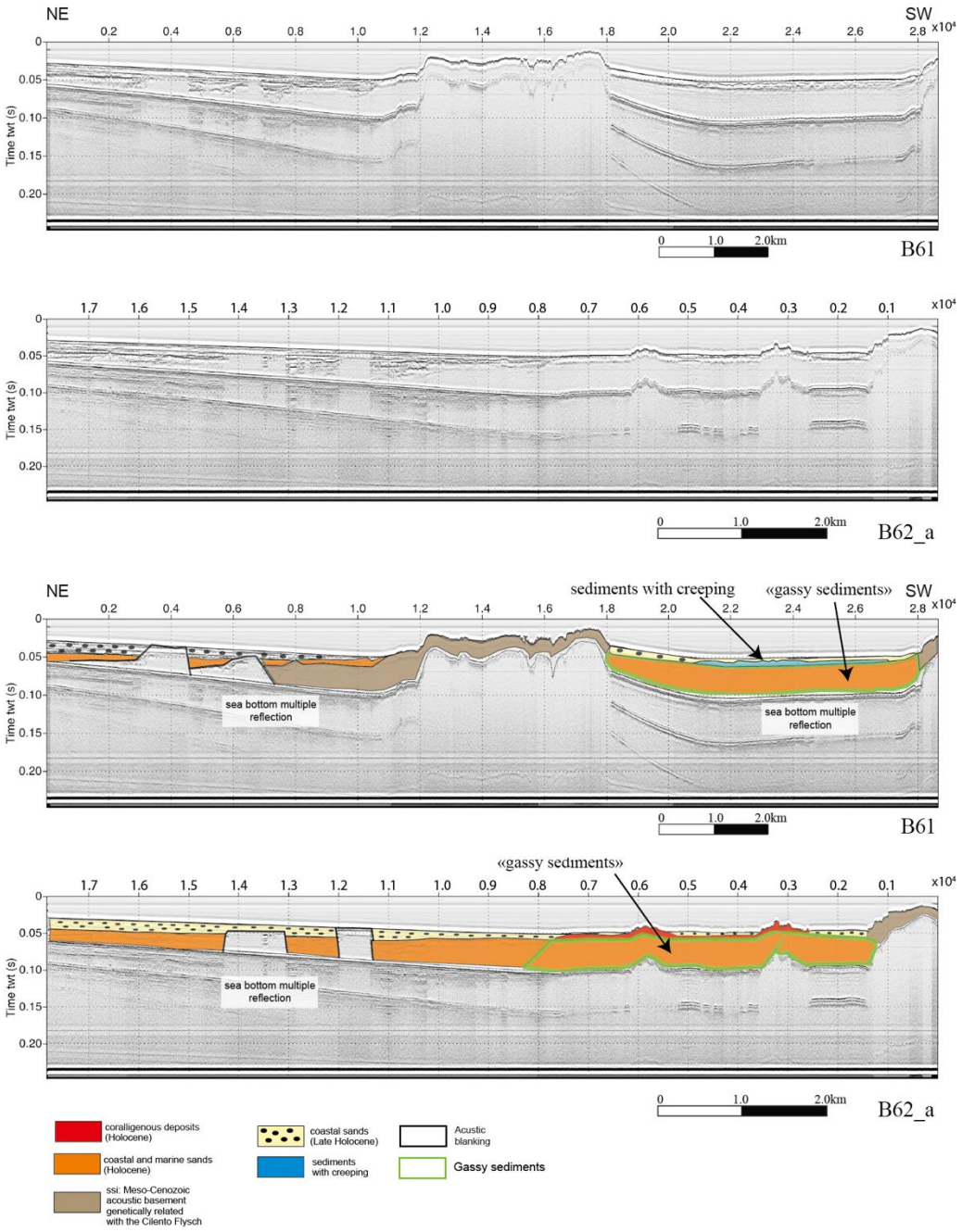

Figure 11. (**top**) Sketch location map of the Sub-bottom chirp profiles of area 3; (**middle**) Sub-bottom chirp profiles B61 and B62_a and the corresponding geologic interpretation (**bottom**).

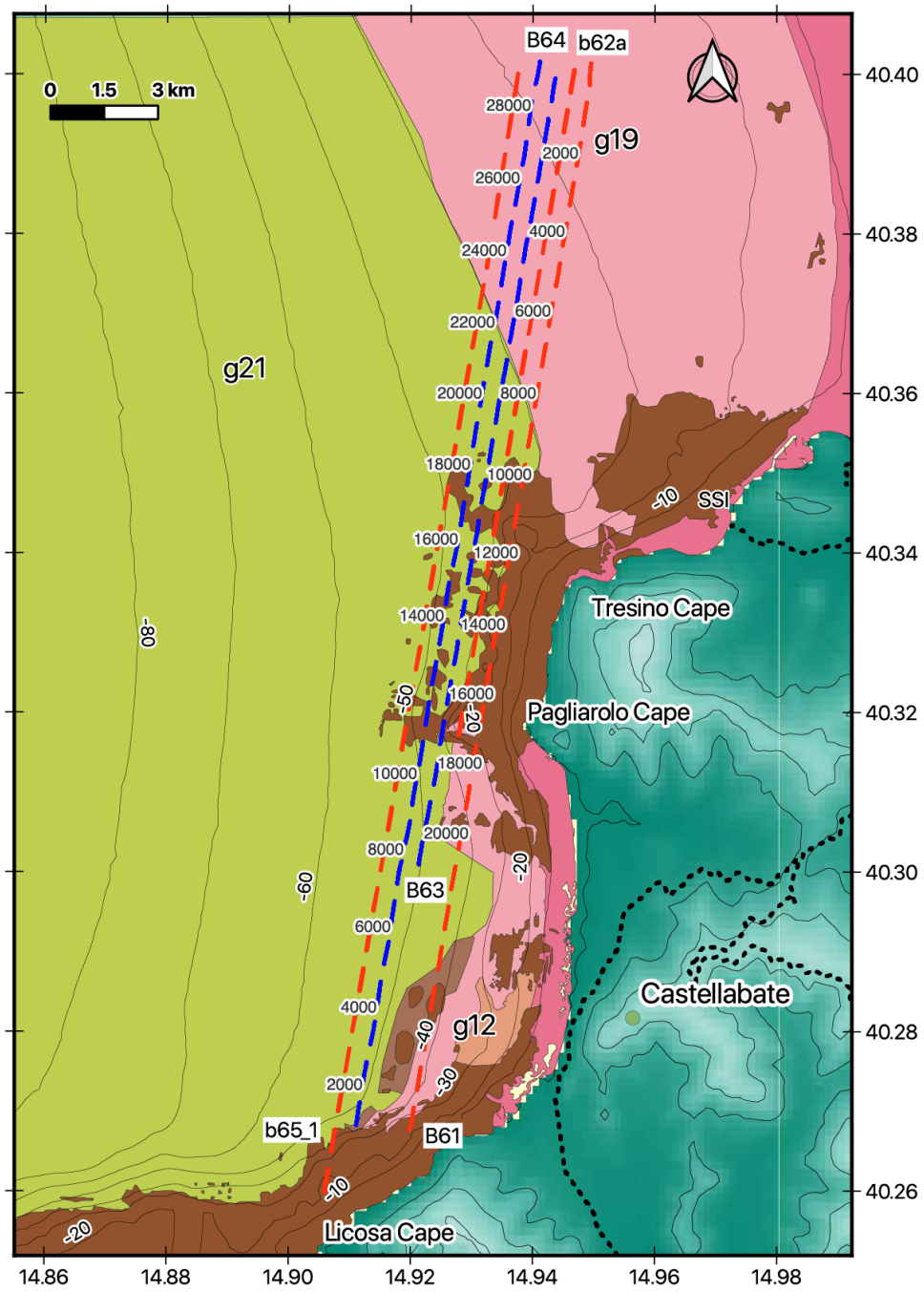

Figure 12. *Cont.*

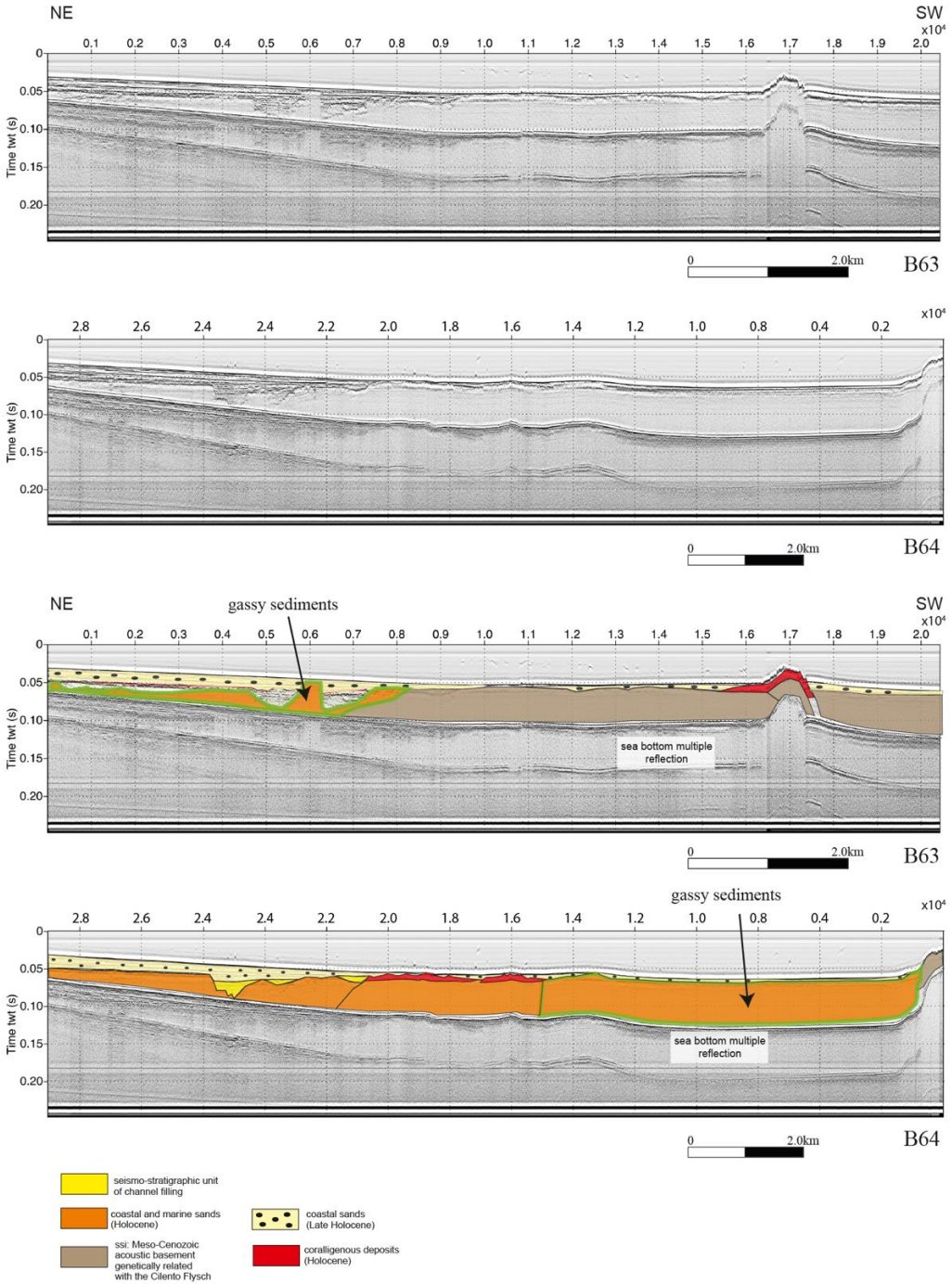

Figure 12. (**top**) Detailed location map; (**middle**) Sub-bottom chirp profiles B63 and B64 and the corresponding geologic interpretation (**bottom**).

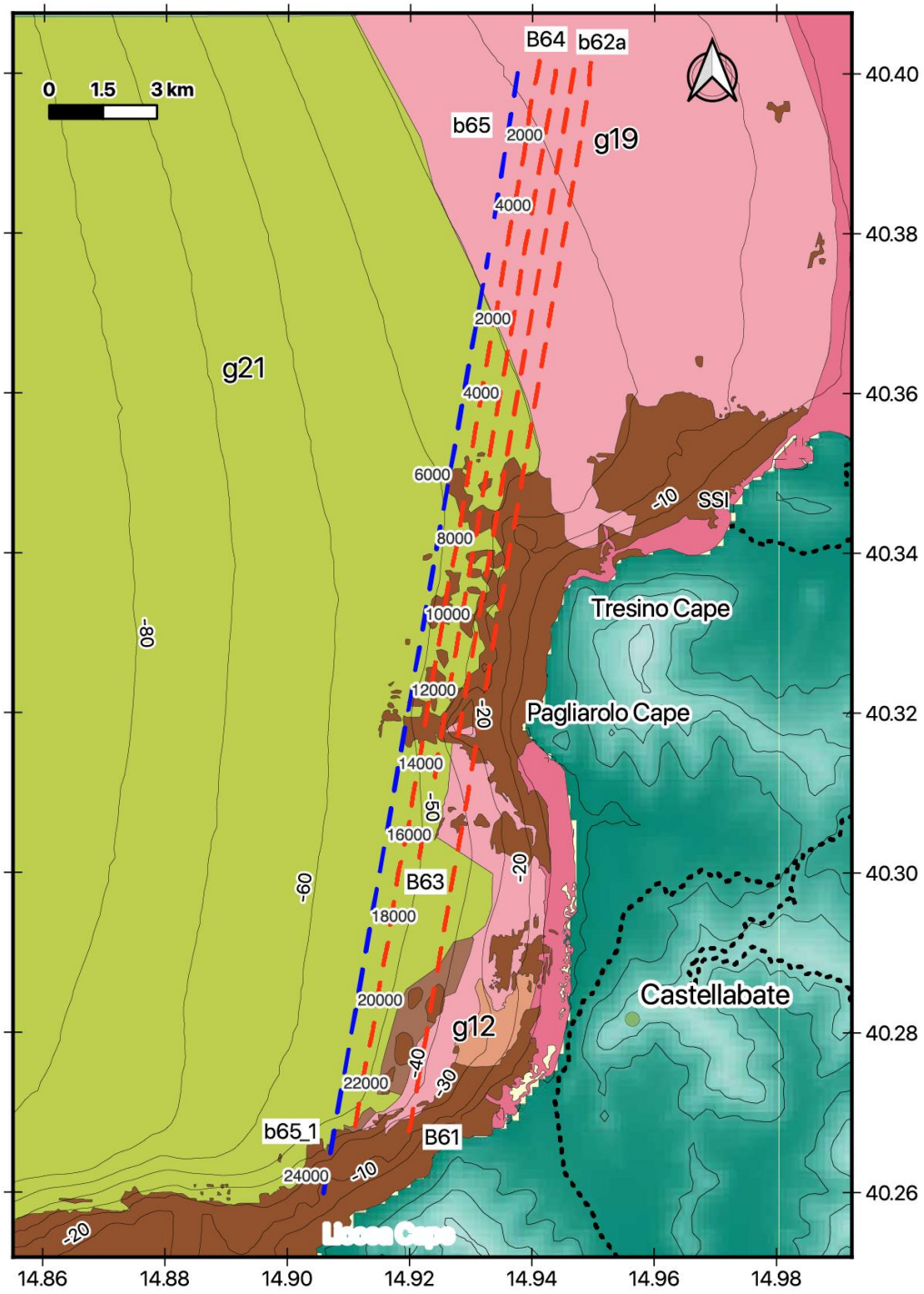

Figure 13. *Cont.*

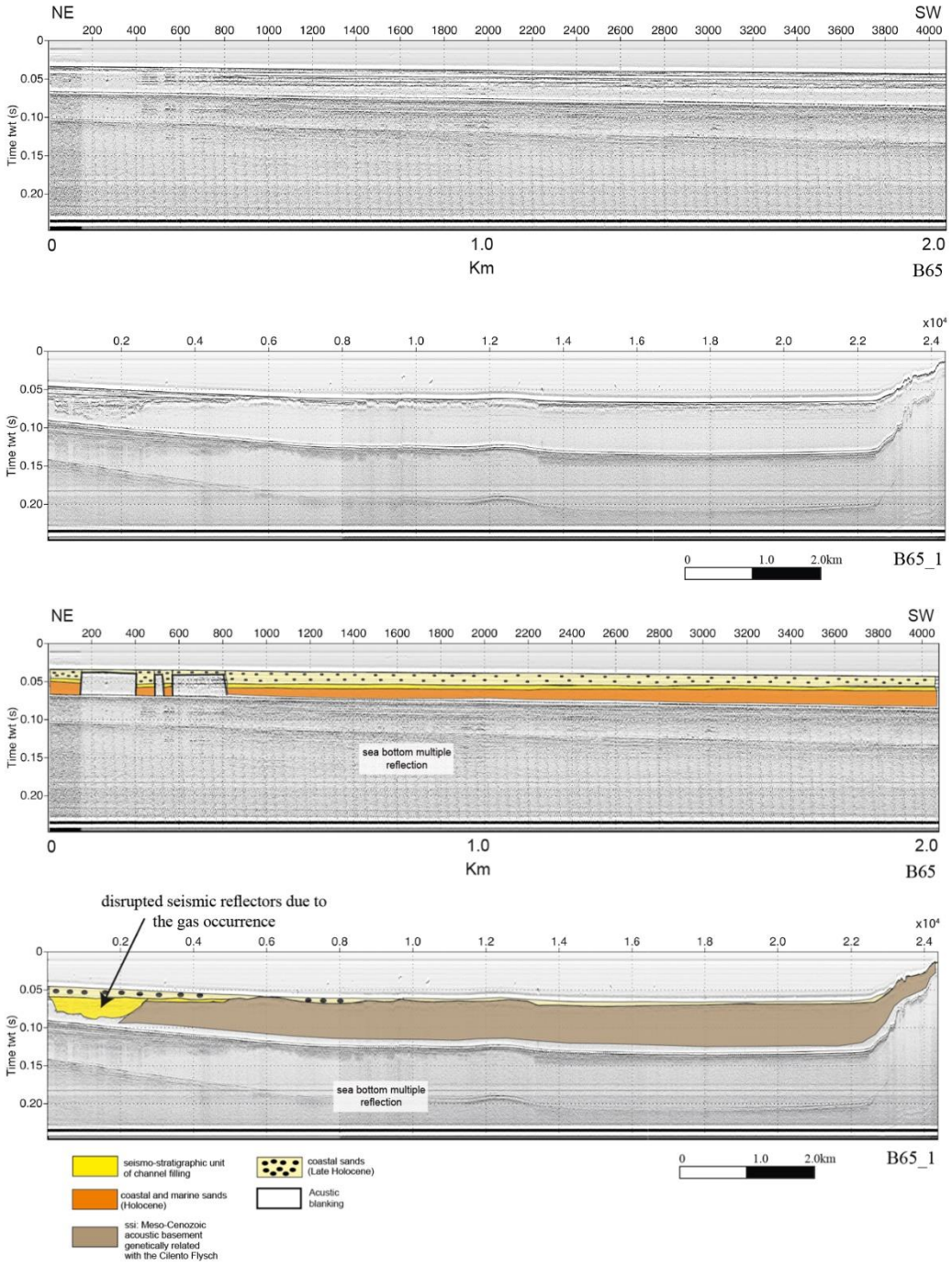

Figure 13. (**top**) Detailed location map; (**middle**) Sub-bottom chirp profiles B65 and B65_1 and the corresponding geologic interpretation (**bottom**).

5. Discussion

The interpretation of the seismoacoustic data has shown that significant gas impregnation affects the Holocene marine deposits, whose stratigraphic architecture is characterized by four or more main seismostratigraphic units overlying the ssi unit, which represents the acoustic basement (Figures 4–13). The number of seismostratigraphic units varies in the three areas distinguished in this paper (Table 1), namely area 1 (Figures 5–7), area 2 (Figures 8–10), and the area 3 (Figures 11–13).

Seismostratigraphic unit 1 is probably composed of sands and overlies the rocky acoustic basement through erosional unconformity. Significant variations in thickness have been observed in correspondence with this unit. These variations could have been

controlled by the occurrence of a rough palaeomorphology, in which unit 1 was deposited. Moreover, strong erosional processes were probably active after the deposition of unit 1, as suggested by the erosional unconformity located at its top, triggering the individuation of the palaeochannels, in which seismostratigraphic 2 was deposited (Figure 4). These filled palaeochannels were observed (Figure 4), from which seismostratigraphic unit 2 is characterized by bidirectional onlaps. The thickness of this unit seems to be quite constant and is in the order of tens of meters. Unit 2 is characterized by acoustically transparent intervals alternating with parallel and continuous seismic reflectors and deposits in the palaeochannels (Figure 4). Seismostratigraphic unit 3 is distinguished by parallel and discontinuous seismic reflectors, interpreted as the first phase of the Holocene basin filling. Seismostratigraphic unit 4 is characterized by a seismic facies with parallel and continuous–discontinuous seismic reflectors, interpreted as the second phase of the Holocene basin filling (Figure 4).

The seismostratigraphic units of area 1 were recognized based on the geological interpretation of the corresponding seismic sections (Figures 5–7). The two main seismostratigraphic units were distinguished, including the ssi unit, which represents the rocky acoustic substratum that is genetically related to the Cilento Flysch, overlain by the recent sedimentary cover. Based on this stratigraphic architecture, it may be suggested that this area represents a structural high whose stratigraphic setting was controlled by the occurrence of the Cilento structural high onshore.

The seismostratigraphic units of area 2 are shown by the corresponding seismic sections (Figures 8–10). Five seismostratigraphic units were distinguished, including the ssi unit, representing the rocky acoustic substratum that is genetically related to the Cilento Flysch, the marine deposits (Holocene in age), the coastal and marine sands (Holocene in age), the seismic sequence filling the palaeochannels, which is correlated with seismostratigraphic unit 2 (previously described), and coastal sands (Holocene in age). Based on this stratigraphic setting, it may be supposed that this area represents a shallow coastal environment, hosting coastal and marine sandy sedimentation spanning the Holocene and Late Holocene. The seismic unit composed of coastal and marine sands, Holocenic in age, is interpreted as gassy sediments.

The seismostratigraphic units of area 3 were interpreted based on the corresponding seismic profiles (Figures 11–13). The six main seismostratigraphic units were distinguished based on seismic interpretation. They include the five seismostratigraphic units of the area 2, while the sixth seismic unit is represented by coralligenous deposits (Holocene in age). Based on this seismostratigraphic setting, this area can be interpreted as a coastal and marine area in which the coralligenous deposits locally grew.

The observed stratigraphic architecture suggests that the inner Cilento continental shelf from the Solofrone River mouth to Agropoli represents a depocenter of marine deposits, showing mainly as sandy grain in size. From Agropoli to the Licosa Cape, the continental shelf clearly represents a structural high. Both from a physiographic and depositional point of view, it is included in the domain of the Licosa Cape morphostructural high. This is highlighted by the wide outcrops of rocky acoustic basement at the sea bottom from Agropoli to the Tresino Cape and from the Tresino Cape to the Pagliarolo Cape. The occurrence of the rocky outcrops has favored the growth of coralligenous deposits, appearing as tabular seismic units cropping out at the sea bottom and overlying the rocky acoustic basement.

The seismic interpretation shows a significant improvement over the seismic data, as processed with the Seismic Unix software, with respect to the same seismic dataset previously processed with the Seisprho software [15]. In fact, the seismic lines processed with Seismic Unix have allowed for the identification of new seismostratigraphic units, including the "gassy sediments" and the coralligenous deposits, among others. These units were not previously distinguished within the seismic data processed using the Seisprho software [15] due to the lower resolution of the seismic data.

The gassy sediments were interpreted as occurring in a wide, acoustically transparent seismic unit (Figures 4–13), represented by coastal and marine sands that are Holocene in age. The characteristics of the gassy sediments have been deeply studied in several areas of the world [11,52–55]. Yuan et al. [52] studied the acoustic and physical characteristics of the gassy sediments in the western Irish Sea based on seismic interpretations of Sub-bottom and Uniboom seismic profiles. Broad areas of acoustic blanking have been highlighted, which were probably controlled by a high content of gas in the fine-grained Holocene sediments. This kind of situation can be compared with the gas-charged sediments occurring in the northern Cilento promontory. These gassy sediments have been basically highlighted in two large areas, with a few smaller pockets in between. Similar to our seismic sections and located in three areas distributed between the northern Cilento Promontory and the Licosa Cape, one of the most predominant acoustic features is represented by acoustic blanking. Seismic and well log evidence have suggested that the gas in the western Irish Sea is probably biogenic in origin and has accumulated in situ in the fine-grained sediments.

Coralligenous deposits were observed in several of the seismic sections in the third area (Figures 11 and 12), outcropping at the sea bottom as localized seismic units and in facies hetheropy with the recent coastal deposits. These kinds of deposits have been recently singled out offshore to the Licosa Cape promontory based on habitat mapping and multibeam bathymetric analysis [17]. It can be suggested that the seismic units observed in Sub-bottom chirp profiles correspond to several coalescent coralligenous bioconstructions (Figures 11 and 12).

In the Cilento offshore area, several acoustic anomalies were identified based on the seismic interpretations. The acoustic features are mainly represented by acoustic blanking, which was mainly detected in the first area, located offshore to the Licosa Cape promontory at water depths ranging between 30 and 90 m (Figure 1), by the shallow gas pockets, which were mainly observed in the second and in the third areas, and by the seismic units impregnated with gas, namely the "gassy" sediments, which were observed both in the second and in the third areas (Table 1). The second and the third areas are located in the northern Cilento promontory from the seaward prolongation of the Paestum Plain, proceeding southwards up to the Tresino Cape, and the third area is located on the northern Cilento promontory, starting from the offshore prolongation of the Paestum Plain up to the Licosa Cape promontory, at water depths ranging between 10 and 60 m (Figure 1).

A sketch map was constructed in order to show the distribution of the acoustic anomalies based on the seismic interpretations (Figure 14). This map was constructed in a GIS environment, mapping the shot points where the main acoustic anomalies were detected based on the seismic interpretations (acoustic blanking, shallow gas pockets, and gassy sediments, see also Table 1). Based on this map, significant acoustic anomalies occur in the depocenter located from the offshore of the Paestum Plain to the Tresino Cape (northern Cilento offshore) and on the outer shelf offshore area to the Licosa Cape. Scattered anomalies occur on the inner shelf offshore to the S. Maria di Castellabate Plain (Figure 14).

The origin of gas in the Cilento offshore area also needs to be discussed. Gas in shallow marine sediments has two main potential sources, including the biogenic gas produced by the bacterial degradation of organic matter at low temperatures and the thermogenic gas produced by the high-temperature degradation and cracking of organic compounds at considerable burial depths [6]. The geology of the study area does not suggest any possible deep thermogenic sources, and it can be hypothesized that the gas has accumulated in situ in the shallow organic-rich sediments. Further core and well log data are required to test this hypothesis since only one core is available from the literature in the study area (Licosa core) [15], but this core has mainly shown relict and palimpsest deposits and organogenic deposits [15]. It is possible that shallow marine and coastal deposits hosted a layer that was rich in organic matter, favoring the development of biogenic gas. In addition, the abundant presence of fine-grained muddy sediments and the high sedimentation rates (resulting in fast burial of the organic matter) also formed an ideal basis for the generation of biogenic gas, but further studies are necessary.

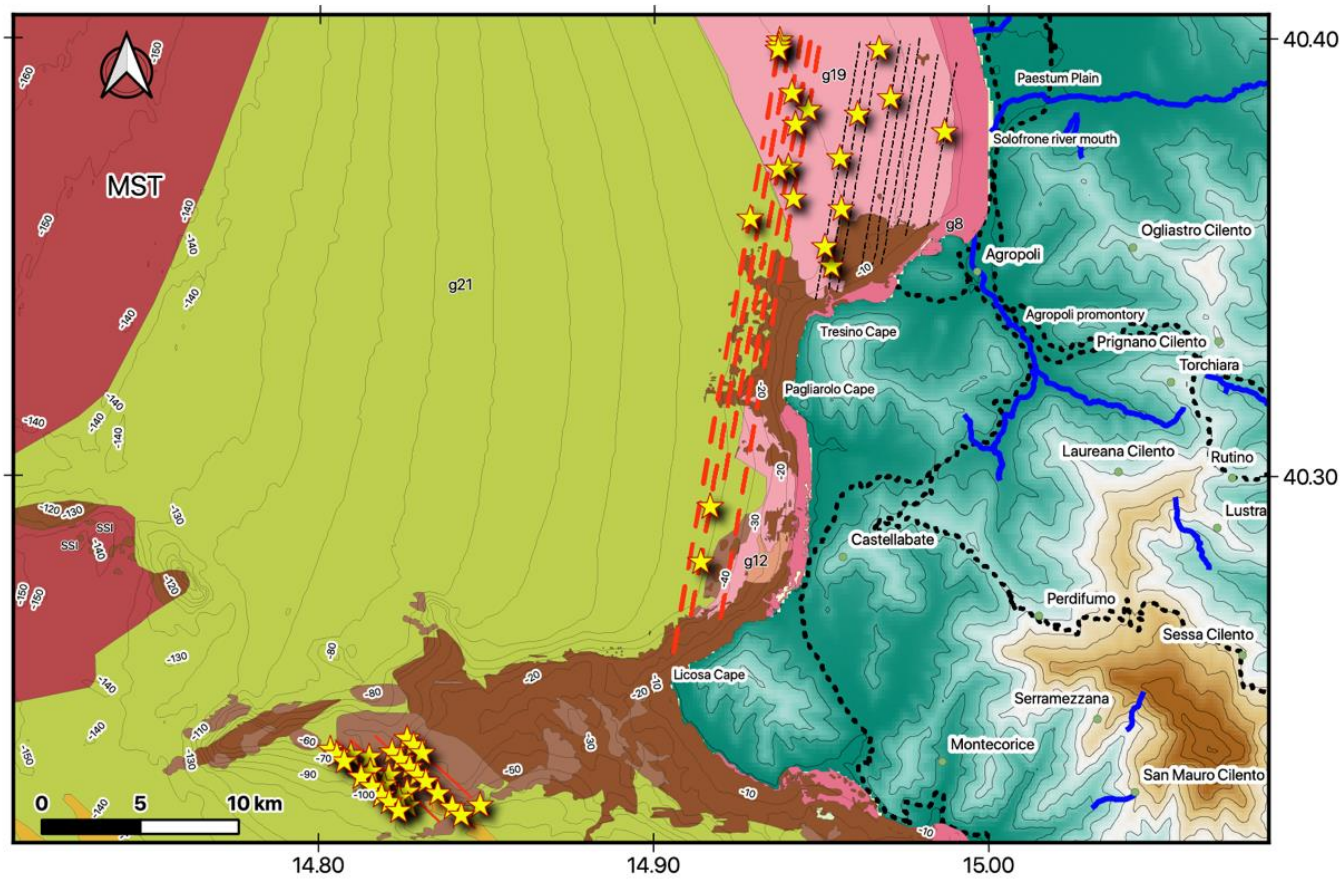

Figure 14. Sketch map showing the distribution of the acoustic anomalies (yellow stars) in the study area based on seismic interpretation.

Literature studies have shown several cases in which the pockmarks are not necessarily associated with the occurrence of shallow gas in the subsurface, as shown by the significant acoustic anomalies identified in the seismic profiles. Missiaen et al. [6] have highlighted that although acoustic blanking locally reaches the surface for the seismic profiles, the seabed morphology does not reveal any clear gas-related features. Hovland and Curzi [9] have shown that acoustic blanking, assumed to represent gas-charged sediments, is not associated with pockmarks but with a locally elevated seabed (mounds or ridges), as controlled by mud diapirism. Hovland and Judd [8] have stated that although acoustic blanking is widespread in the North Sea, including the pockmark areas, it is not ubiquitous, neither is it always found in close association with pockmarks. In the present work, the whitened band on the seismic profiles does not arrive at the seafloor; it arrives at the seabed only locally. This should mean that the gas does not escape into the water column that generates the pockmarks; these features are not present in the high-resolution bathymetry [17]. In that case, the pockmarks are not associated with the occurrence of gas in the Cilento offshore area, but buried gassy sediments have been detected. A number of studies on the subject under consideration using modern software exist. Among them, a significant study has been recently carried out by Bosikov and Klyuev [56], highlighting that the use of modern computer-aided methods, in particular the use of the Micromine software, is an important part of the integrated research for the determination of deposit prospects for various ores. This study has analyzed the prospects and estimation of reserves for open-pit and underground mining in the Berezkinskoye ore field, demonstrating the high potentiality of modern software, as it was in this paper.

The occurrence of gas in the Campania offshore area is not novel. Important structures linked to gas occurrence have been previously described in the Campania region, in

particular, the offshore of the Volturno River mouth. Distinct sites of vertically focused flows, marked by columnar zones of amplitude that mask and disrupt reflectors, reached the seabed at the outer shelf and corresponded with the alignment of elongated pockmarks [57]. In that case, acoustic anomalies are associated with pockmarks.

6. Conclusions

High-resolution seismoacoustic data provide an appropriate technique for studying gas-charged sediments through the recognition of the diagnostic intrasedimentary features associated with the occurrence of gas in marine deposits.

The acoustic anomalies of the Cilento offshore area were studied based on the geological interpretation of Sub-bottom chirp profiles. Acoustic blanking, shallow gas pockets, and gassy sediments, occurring as wide, acoustically transparent seismic units, were identified in the study area. The occurrence of these features, however, suggests that the northern Cilento promontory represents an interesting area whose features need to be studied in more detail in subsequent research in order to relate these relationships with marine geohazards.

A processing sequence was constructed by using the Seismic Unix software and was applied to the seismic record in order to highlight acoustic anomalies, indicating the occurrence of Quaternary marine deposits that are impregnated with gas. A new processing sequence for high-resolution seismic data was applied to Sub-bottom seismic profiles located in the northern Cilento offshore area by using Seismic Unix software [14]. The workflow allowed us to plot the Sub-bottom profiles using Seismic Unix, therefore obtaining high-resolution seismic sections. This processing sequence has allowed for a significant improvement in the seismic profiles with respect to the previous versions obtained through Seisprho (Figure 4) [15].

A sketch morphobathymetric map was constructed through GIS (Geographic Information System) in order to show the morphostructural features of the study area. These features consist of the outcrops of the rocky acoustic basement (ssi unit), sandy ridges–representing relict and palimpsest deposits occurring both northwestwards and southwestwards of the Licosa Cape promontory–channels, and abrasion terraces. This map has been integrated into another map and constructed in the GIS environment, reporting the location of the main acoustic anomalies of the Cilento offshore area based on seismic interpretation.

In the Cilento offshore area, three areas were distinguished, typified by different acoustic features (Figure 1; Table 1). In the first area, located offshore from the Licosa Cape at between 30 and 90 m of water depth, the distinctive acoustic feature is represented by acoustic blanking controlled by the occurrence of gas [6,7]. The second area is in the northern Cilento promontory, from the seaward prolongation of the Paestum Plain to the Tresino Cape, and the distinctive acoustic features are represented by shallow gas pockets. The third area is located on the northern Cilento promontory, from the offshore prolongation of the Paestum Plain up to the Licosa Cape at water depths ranging between 10 and 60 m; the distinctive acoustic features are represented by shallow gas pockets and by the seismic units impregnated by gas ("gassy sediments").

The seismostratigraphic setting of the Cilento offshore area was reconstructed based on the geological interpretation of Sub-bottom chirp profiles, highlighting the different seismostratigraphic units of the three areas. While the first area represents a structural high, the second and the third areas represent shallow coastal and marine environments, where coralligenous deposits locally grew. In this geologic setting, and taking into account similar case histories, we may suppose that the gas is biogenic in origin, but further studies are necessary.

Author Contributions: Conceptualization, G.A. and M.C.; methodology, M.C.; software, M.C.; formal analysis, G.A.; investigation, G.A.; data curation, M.C.; writing—original draft preparation, G.A.; writing—review and editing, G.A. All authors have read and agreed to the published version of the manuscript.

Funding: This research received no external funding.

Institutional Review Board Statement: Not applicable.

Informed Consent Statement: Not applicable.

Data Availability Statement: Not applicable.

Conflicts of Interest: The authors declare no conflict of interest.

References

1. Carlson, P.R.; Golan-Bac, M.; Karl, H.A.; Kvenvolden, K.A. Seismic and geochemical evidence for shallow gas in sediment of Navarin continental margin, Bering Sea. *AAPG Bull.* **1985**, *69*, 422–436.
2. Judd, A.G.; Hovland, M. The evidence of shallow gas in marine sediments. *Continent. Shelf Res.* **1992**, *12*, 1081–1095. [CrossRef]
3. Lee, S.H.; Chough, S.K. Distribution and origin of shallow gas in deep-sea sediments of the Ulleung Basin, East Sea (Sea of Japan). *Geo-Mar. Lett.* **2003**, *22*, 204–209. [CrossRef]
4. Hovland, M. The Geomorphology and Nature of Seabed Seepage Processes. In *Bathymetry and Its Applications*; Blondel, P., Ed.; IntechOpen: Rjeka, Croatia, 2012; Chapter 4; pp. 79–104.
5. Heggland, R. Gas seepage as an indicator of deeper prospective reservoirs. A study based on exploration 3D seismic data. *Mar. Petrol. Geol.* **1998**, *15*, 1–9. [CrossRef]
6. Missiaen, T.; Murphy, S.; Loncke, L.; Henriet, J.P. Very high-resolution seismic mapping of shallow gas in the Belgian coastal zone. *Cont. Shelf Res.* **2002**, *22*, 2291–2301. [CrossRef]
7. Andreassen, K.; Espen, G.; Nilssen, E.G.; Ødegaard, C.M. Analysis of shallow gas and fluid migration within the Plio-Pleistocene sedimentary succession of the SW Barents Sea continental margin using 3D seismic data. *Geo-Mar. Lett.* **2007**, *27*, 155–171. [CrossRef]
8. Hovland, M.; Judd, A.G. *Seabed Pockmarks and Seepages: Impact on Geology, Biology and the Marine Environment*; Graham and Trotman: London, UK, 1988; p. 293.
9. Hovland, M.; Curzi, P.V. Gas seepage and assumed mud diapirism in the Italian central Adriatic Sea. *Mar. Petrol. Geol.* **1989**, *6*, 161–169. [CrossRef]
10. Geletti, R.; Del Ben, A.; Busetti, M.; Ramella, R.; Volpi, V. Gas seeps linked to salt structures in the Central Adriatic Sea. *Basin Res.* **2008**, *20*, 473–487. [CrossRef]
11. Spatola, D.; Micallef, A.; Sulli, A.; Basilone, L.; Basilone, G. Evidence of active fluid seepage (AFS) in the southern region of the central Mediterranean sea. *Measurement* **2018**, *128*, 247–253. [CrossRef]
12. Ceramicola, S.; Dupré, S.; Somoza, L.; Woodside, J. Cold seep systems. In *Submarine Geomorphology*; Micallef, A., Krastel, S., Savini, A., Eds.; Springer International Publishing: Cham, Switzerland, 2018; pp. 367–387.
13. Kopp, H.; Chiocci, F.L.; Berndt, C.; Çağatay, M.N.; Ferreira, T.; Fortes, C.J.E.M.; Gràcia, E.; González Vega, A.; Kopf, A.J.; Sørensen, M.B.; et al. Marine geohazards: Safeguarding society and the Blue Economy from a hidden threat. In *Position Paper 26 of the European Marine Board*; Muñiz Piniella, A., Kellett, P., van den Brand, R., Alexander, B., Rodríguez Perez, A., Van Elslander, J., Heymans, J.J., Eds.; European Marine Board: Ostend, Belgium, 2021; p. 100.
14. Colorado School of Mines. Seismic Unix. 2000. Available online: https://wiki.seismic-unix.org (accessed on 30 October 2022).
15. Aiello, G.; Caccavale, M. The Depositional Environments in the Cilento Offshore (Southern Tyrrhenian Sea, Italy) Based on Marine Geological Data. *J. Mar. Sci. Eng.* **2021**, *9*, 1083. [CrossRef]
16. Gasperini, L.; Stanghellini, G. SEISPRHO: An interactive computer program for processing and interpretation of high-resolution seismic reflection profiles. *Comput. Geosci.* **2009**, *35*, 1497–1507. [CrossRef]
17. Violante, C. Computer-Aided Geomorphic Seabed Classification and Habitat Mapping at Punta Licosa MPA, Southern Italy. In *ICCSA 2020: Computational Science and Its Applications*; Gervasi, O., Morgante, B., Misra, S., Garau, C., Blecic, I., Tanion, D., Apduhan, B.O., Rocha, A., Tarantino, E., Torre, C., et al., Eds.; Springer Nature: Bern, Switzerland, 2020; pp. 681–695.
18. Ortolani, F.; Aprile, F. Nuovi dati sulla struttura profonda della Piana Campana a sud-est del fiume Volturno. *Boll. Soc. Geol. Ital.* **1978**, *97*, 591–608.
19. Fabbri, A.; Gallignani, P.; Zitellini, N. Geologic evolution of the peri-Tyrrhenian sedimentary basins. In *Sedimentary Basins of Mediterranean Margins*; Wezel, F.C., Ed.; Tecnoprint: Bologna, Italy, 1981; pp. 101–126.
20. Bartole, R. Tectonic structure of the Latian-Campanian shelf (Tyrrhenian Sea). *Boll. Oceanol. Teor. Appl.* **1984**, *2*, 197–230.
21. Bartole, R.; Savelli, D.; Tramontana, M.; Wezel, F.C. Structural and sedimentary features in the Tyrrhenian margin off Campania, Southern Italy. *Mar. Geol.* **1983**, *55*, 163–180. [CrossRef]
22. Finetti, I.; Morelli, C. Esplorazione sismica per riflessione dei Golfi di Napoli e Pozzuoli. *Boll. Geof. Teor. Appl.* **1973**, *16*, 175–222.
23. Trincardi, F.; Zitellini, N. The rifting of the Tyrrhenian Basin. *Geo-Mar. Lett.* **1987**, *7*, 1–6. [CrossRef]
24. Mariani, M.; Prato, R. I bacini neogenici del margine tirrenico: Approccio sismico-stratigrafico. *Mem. Soc. Geol. Ital.* **1988**, *41*, 519–531.
25. Aiello, G.; Marsella, E.; Sacchi, M. Quaternary structural evolution of Terracina and Gaeta basins (Eastern Tyrrhenian margin, Italy). *Rend. Lincei* **2000**, *11*, 41–58. [CrossRef]

26. Aiello, G.; Marsella, E.; Cicchella, A.G.; Di Fiore, V. New insights on morpho-structures and seismic stratigraphy along the Campania continental margin (Southern Italy) based on deep multichannel seismic profiles. *Rend. Lincei* **2011**, *22*, 349–373. [CrossRef]
27. Aiello, G.; Cicchella, A.G.; Di Fiore, V.; Marsella, E. New seismo- stratigraphic data of the Volturno Basin (northern Campania, Tyrrhenian margin, southern Italy): Implications for tectono-stratigraphy of the Campania and Latium sedimentary basins. *Ann. Geophys.* **2011**, *54*, 265–283.
28. Aiello, G.; Iorio, M.; Molisso, F.; Sacchi, M. Integrated morpho-bathymetric, seismic stratigraphic and sedimentological data on the Dohrn canyon (Naples Bay, Southern Tyrrhenian Sea): Relationships with volcanism and tectonics. *Geosciences* **2020**, *10*, 319. [CrossRef]
29. Conti, A.; Bigi, S.; Cuffaro, M.; Doglioni, C.; Scrocca, D.; Muccini, F.; Cocchi, L.; Ligi, M.; Bortoluzzi, G. Transfer zones in an oblique back-arc basin setting: Insights from the Latium-Campania segmented margin (Tyrrhenian Sea). *Tectonics* **2017**, *36*, 78–107. [CrossRef]
30. Zitellini, N.; Ranero, C.R.; Loreto, M.F.; Ligi, M.; Pastore, M.; D'Oriano, F.; Sallares, V.; Grevemeyer, I.; Moeller, S.; Prada, M. Recent inversion of the Tyrrhenian Basin. *Geology* **2020**, *48*, 123–127. [CrossRef]
31. Doglioni, C. A proposal for the kinematic modelling of the Tyrrhenian-Apennines system. *Terra Nova* **1991**, *3*, 423–432. [CrossRef]
32. Spadini, G.; Wezel, F.C. Structural evolution of the "41st parallel zone": Tyrrhenian Sea. *Terra Nova* **1994**, *6*, 552–562. [CrossRef]
33. Carminati, E.; Wortel, M.J.R.; Spakman, W.; Sabadini, R. The role of slab detachment processes in the opening of the western central Mediterranean basins: Some geological and geophysical evidence. *Earth Planet. Sci. Lett.* **1998**, *160*, 651–665. [CrossRef]
34. Bruno, P.P.G.; Di Fiore, V.; Ventura, G. Seismic study of the '41st Parallel' Fault System offshore the Campanian–Latial continental margin, Italy. *Tectonophysics* **2000**, *324*, 37–55. [CrossRef]
35. Faccenna, C.; Becker, T.W.; Lucente, F.P.; Jolivet, L.; Rossetti, F. History of subduction and back-arc extension in the Central Mediterranean. *Geophys. J. Intern.* **2001**, *145*, 809–820. [CrossRef]
36. Billi, A.; Bosi, V.; De Meo, A. Caratterizzazione strutturale del rilievo del Monte Massico nell'ambito dell'evoluzione quaternaria delle depressioni costiere dei fiumi Garigliano e Volturno. (*Campania settentrionale*). *IL Quaternario* **1997**, *10*, 15–26.
37. Santangelo, N.; Romano, P.; Ascione, A.; Russo Ermolli, E. Quaternary evolution of the Southern Apennines coastal plains: A review. *Geol. Carpathica* **2017**, *68*, 43–56. [CrossRef]
38. Aiello, G.; Cicchella, A.G. Dati sismostratigrafici sul margine continentale della Campania tra Ischia, Capri ed il Bacino del Volturno (Tirreno meridionale, Italia) in base al processing sismico ed all'interpretazione geologica di profili sismici a riflessione multicanale. *Quad. Geofis.* **2019**, *149*, 1–52. (In Italian)
39. D'Argenio, B.; Pescatore, T.; Scandone, P. *Schema Geologico dell'Appennino Meridionale*; Verlag: Berlin, Germany; Volume 183, pp. 49–72.
40. Mostardini, F.; Merlini, S. Appennino centro-meridionale. Sezioni Geologiche e Proposta di Modello Strutturale. *Mem. Soc. Geol. Ital.* **1986**, *35*, 177–202.
41. Vitale, S.; Ciarcia, S. Tectono-stratigraphic setting of the Campania region (southern Italy). *J. Maps* **2018**, *14*, 9–21. [CrossRef]
42. Amore, F.O.; Bonardi, G.; Ciampo, G.; De Capoa, P.; Perrone, V.; Sgrosso, I. Relazioni tra flysch interni e domini appenninici: Reinterpretazione delle formazioni di Pollica, S. Mauro e Albidona e l'evoluzione infra-medio-miocenica delle zone esterne sud appenniniche. *Mem. Soc. Geol. Ital.* **1988**, *41*, 285–297.
43. Bonardi, G.; Amore, F.O.; Ciampo, G.; De Capoa, P.; Miconnet, P.; Perrone, V. Il Complesso Liguride *Auct*.: Stato delle conoscenze e problemi aperti sulla sua evoluzione pre-appenninica ed i suoi rapporti con l'Arco Calabro. *Mem. Soc. Geol. Ital.* **1988**, *41*, 7–35.
44. Zuppetta, A.; Mazzoli, S. Deformation history of a synorogenic sedimentary wedge, northern Cilento area, southern Apennines thrust and fold belt, Italy. *GSA Bull.* **1997**, *109*, 698–708. [CrossRef]
45. Cammarosano, A.; Cavuoto, G.; Martelli, L.; Nardi, G.; Toccaceli, R.M.; Valente, A. Il Progetto CARG nell'area silentina (area interna Appennino meridionale): Il nuovo assetto stratigrafico-strutturale derivante dal rilevamento dei fogli 503, 502, e 519 (Vallo della Lucania, Agropoli e Capo Palinuro). *Rend. Online Soc. Geol. Ital.* **2011**, *12*, 19–21.
46. Aiello, G.; Di Fiore, V.; Marsella, E.; D'Isanto, C. Stratigrafia sismica e morfobatimetria della Valle di Salerno. In Proceedings of the 26th National Congress GNGTS (Gruppo Nazionale di Geofisica della Terra Solida), Rome, Italy, 24–27 November 2007; Extended Abstract. pp. 495–498.
47. Aiello, G.; Marsella, E.; Di Fiore, V.; D'Isanto, C. Stratigraphic and structural styles of half-graben offshore basins: Multichannel seismic and Multibeam morpho-bathymetric evidences on the Salerno Valley (Southern Campania continental margin, Italy). *Quad. Geofis.* **2009**, *77*, 1–34. (In English)
48. Aiello, G.; Sacchi, M. New morpho-bathymetric data on marine hazard in the offshore of Gulf of Naples (Southern Italy). *Nat. Hazards* **2022**, *111*, 2881–2908. [CrossRef]
49. Vail, P.R.; Mitchum, R.M.; Thompson, S. Seismic stratigraphy and global changes of sea level, part IV: Global cycles of relative changes of sea level. In *Seismic Stratigraphy—Applications to Hydrocarbon Exploration*; Memoir 26; Payton, C.E., Ed.; American Association of Petroleum Geologists: Tulsa, OK, USA, 1977; pp. 83–98.
50. Mitchum, R.M.; Vail, P.R.; Thompson, S. Seismic stratigraphy and global changes of sea-level, part 2: The depositional sequence as a basic unit for stratigraphic analysis. In *Seismic Stratigraphy—Applications to Hydrocarbon Exploration*; Memoir 26; Payton, C.E., Ed.; American Association of Petroleum Geologists: Tulsa, OK, USA, 1977; pp. 53–62.

51. Anstey, N.A. *Simple Seismics: For the Petroleum Geologist, the Reservoir Engineer, the Well-Log Analyst, the Processing Technician, and the Man in the Field*; Heathfield: East Sussex, England, 1982; p. 168.
52. Yuan, F.; Bennell, J.D.; Davis, A.M. Acoustic and physical characteristics of gassy sediments in the western Irish sea. *Continent. Shelf Res.* **1992**, *12*, 1121–1134. [CrossRef]
53. Fleischer, P.; Orsi, T.H.; Richardson, M.D.; Anderson, A.L. Distribution of free gas in marine sediments: A global overview. *Geo-Mar. Lett.* **2001**, *21*, 103–122.
54. Gorgas, T.J.; Kim, G.Y.; Park, S.C.; Wilkens, R.H.; Kim, D.C.; Lee, G.H.; Seo, Y.K. Evidence for gassy sediments on the inner shelf of SE Korea from geoacoustic properties. *Continent. Shelf Res.* **2003**, *23*, 821–834. [CrossRef]
55. Leighton, T.G.; Robb, G.B.N. Preliminary mapping of void fractions and sound speeds in gassy marine sediments from subbottom profiles. *J. Acoust. Soc. Am.* **2008**, *124*, EL313–EL320. [CrossRef] [PubMed]
56. Bosikov, I.I.; Klyuev, R.V. Assessment of Berezkinskoye ore field prospectivity using Micromine software. *Geol. Miner. Depos.* **2022**, *7*, 192–202. [CrossRef]
57. Misuraca, M.; Budillon, F.; Tonielli, R.; Di Martino, G.; Innangi, S.; Ferraro, L. Coastal Evolution, Hydrothermal Migration Pathways and Soft Deformation along the Campania Continental Shelf (Southern Tyrrhenian Sea): Insights from High-Resolution Seismic Profiles. *Geosciences* **2018**, *21*, 121. [CrossRef]